Phonons in Graphene and van der Waals Materials

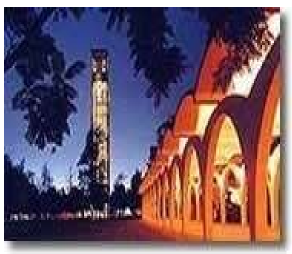

Alexander A. Balandin

Department of Electrical Engineering and
Materials Science and Engineering Program
University of California – Riverside

MRS Medal Talk
Fall 2013

NRI nanoelectronics RESEARCH INITIATIVE

FENA ONR Office of Naval Research NSF STARnet SRC DARPA FAME

Nano-Device Laboratory (NDL)
Department of Electrical Engineering
University of California – Riverside

| Nano-Device Laboratory >

Profile: experimental and theoretical research in advanced materials and nano-devices

PI: Alexander A. Balandin

Thermal and Electrical Characterization

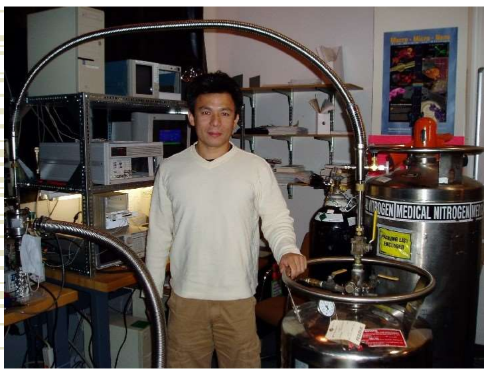

Device Design and Characterization

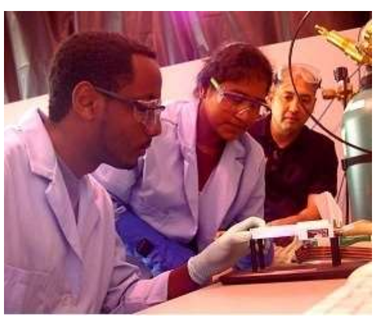

Phononics Research & Applications

Electronic Devices and Circuits

Direct Energy Conversion

Optoelectronics

Bio-Nanotech

Nanoscale Characterization

Theory and Modeling

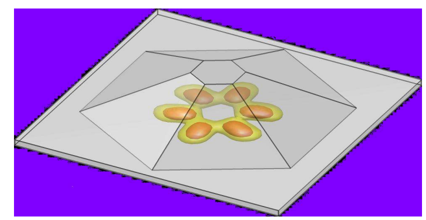

Raman, Fluorescence and PL Spectroscopy

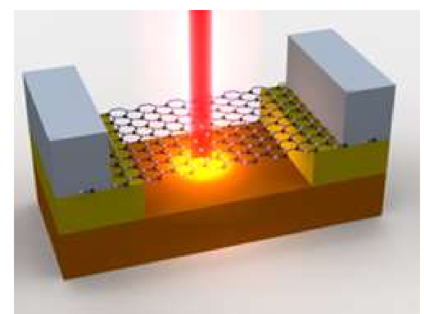

Outline

- *Introduction and Basic Definitions*
  - *Phonons*
  - *Thermal conductivity*
- *Thermal Conductivity of Graphene*
  - *Raman spectroscopy*
  - *Optothermal technique*
  - *Theoretical interpretation*
- *Graphene Thermal Applications*
  - *TIMs and PCMs*
  - *Heat spreaders*
- *Phonons in van der Waals Materials*
  - *Raman metrology*
  - *Charge-density waves*
- *Outlook: Phononics and Phonon Engineering*

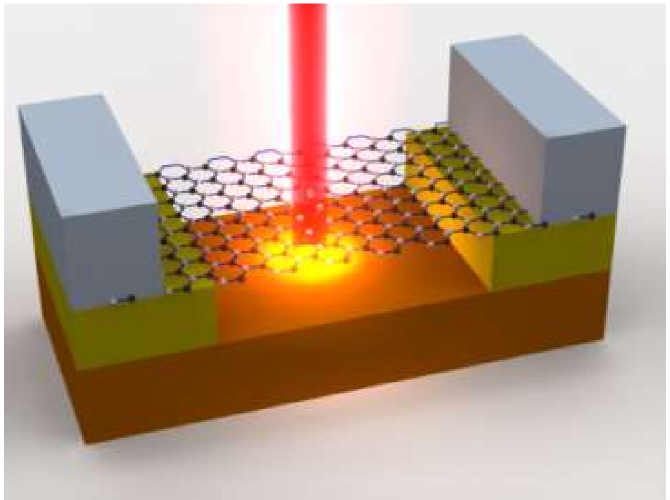

Practical Motivations: Why Material Scientists Should Study Thermal Properties?

IEEE Spectrum illustration of the thermal issues in the feature article *Chill Out: New Materials and Designs Can Keep Chips Cool* by A.A. Balandin.

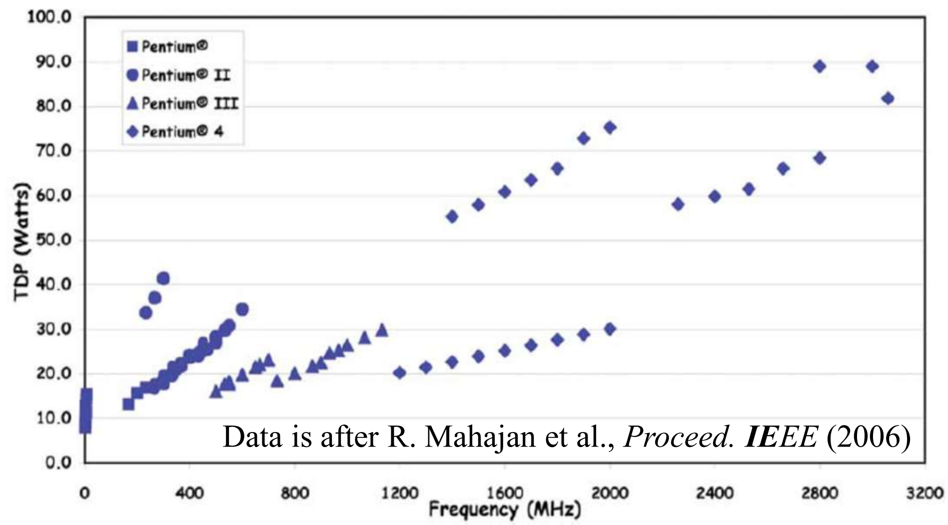

No BIG fan solutions!

→The switch to multi-core designs alleviates the growth in the thermal design power (TDP) increase but does not solve the hot-spot problem

→ Non-uniform power densities leading to hot-spots (>500 W/cm^2)

Basics of Pho*n*ons

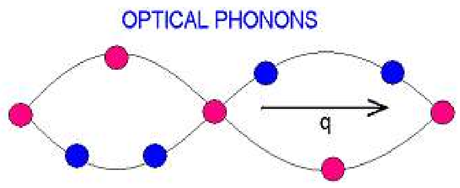

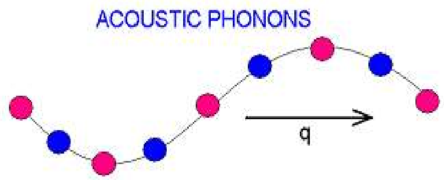

Bose-Einstein statistics:

$$<n_\omega> = \frac{1}{\exp\left\{\frac{\hbar\omega}{k_B T}\right\} - 1}$$

$E_{LO,TO}$(Si)=64.3 meV (Γ point)
$E_{LO,TO}$(Ge)=37.2 meV (Γ point)
V_L(Si)=8433 m/s; V_T(Si)=5845 m/s

g-atoms/unit cell → 3g modes per **q** value: 3 acoustic and 3(g-1) optical

The quantum of the energy of a lattice vibration is called a phonon in analogy with the photon of the electromagnetic wave.

Bulk Semiconductor

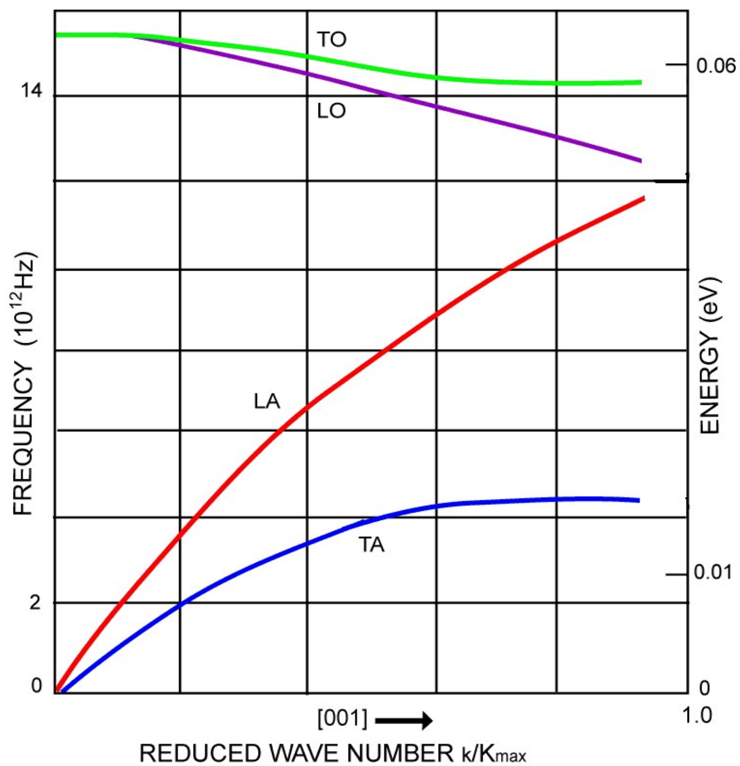

Phonons affect thermal, electrical and optical phenomena in semiconductors

Heat is carried by acoustic phonons

Electron mobility is limited by phonons

Optical response is affected by phonons

Electronic noise is influenced by phonons

Basics of Thermal Conductivity

Definitions and Basic Theory

Fourier's law:

$$\frac{\dot{Q}}{S} = -K\nabla T$$

Phonon vs. electron conduction:

$$\frac{K_e}{\sigma} = \frac{\pi^2}{3}\left(\frac{k_B}{e}\right)^2 T$$

Heat current carried by phonons :

$$Q = \sum_{q,j} N_{\mathbf{q},i}(\mathbf{q})\hbar\omega_i(\mathbf{q})\frac{\partial\omega}{\partial\mathbf{q}},$$

RT thermal conductivity of important materials:

Silicon (Si): 145 W/mK

SiO_2: 0.5 – 1.4 W/mK

Copper: 385 - 400 W/mK

RT thermal conductivity for carbon materials:

Diamond: 1000 – 2200 W/mK

Graphite: 20 – 2000 W/mK (orientation)

DLC: 0.1 – 10 W/mK

CNTs: 3000 – 3500 W/mK

→ Very wide range of K for carbon materials depending on their lattice and dimensionality

Thermal Conductivity of Bulk Carbon Materials

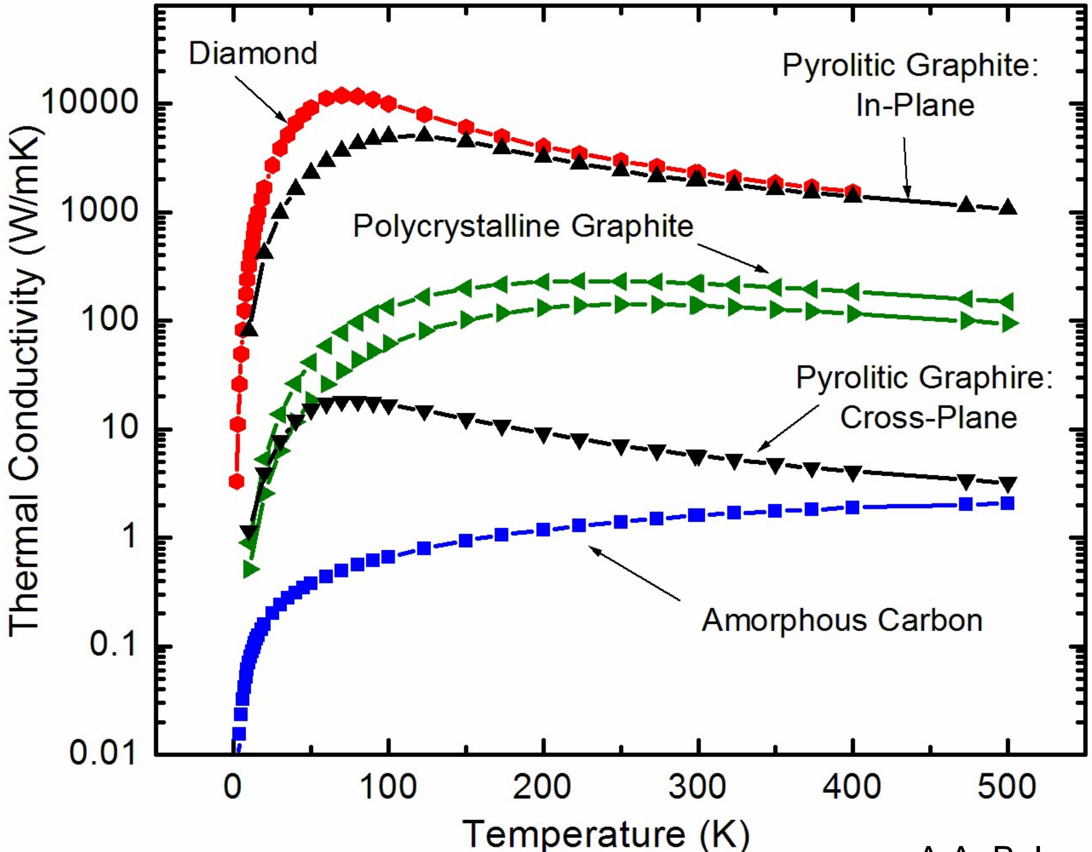

← Curves are plotted with "recommended" values from multiple sources.

← Bulk graphite: 2000 W/mK at RT

← Order of magnitude difference in high-quality graphite depending on the method and polycrystallinity

A.A. Balandin, "Thermal properties of graphene and nanostructured carbon materials," Nature Materials, 10, 569 - 581 (2011).

Degradation of Thermal Conductivity of Thin Films: Extrinsic Phonon Transport Regime

Thermal conductivity usually decreases as one goes from bulk material to nanostructure or thin film

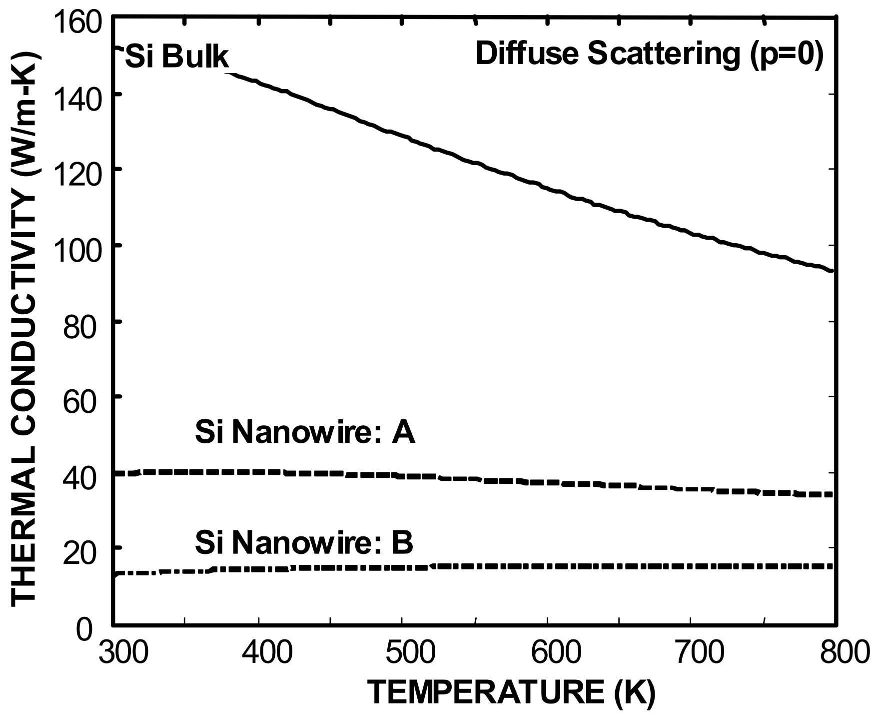

J. Zou and A.A. Balandin, *J. Appl. Phys.*, **89**, 2932 (2001).

←Thermal conductivity of bulk Si at room temperature: K= 148 W/m-K

← Thermal conductivity of Si nanowire with cross section of 20 nm x 20 nm: K=13 W/mK

→ Phonon thermal conductivity:

$$K_p = (1/3)C_p \upsilon\ \Lambda$$

→ Boundary-limited MFP ($\Lambda = v\tau$):

$$\frac{1}{\tau_B} = \frac{\upsilon}{D}\frac{1-p}{1+p}$$

$$K_p \sim C_p \upsilon \Lambda \sim C_p \upsilon^2 \tau_B \sim C_p \upsilon D$$

Thermal Conductivity of 2D Crystals in Intrinsic Phonon Transport Regime: *Infinity*

- → The momentum conservation in 1D and 2D systems with anharmonicity leads to the divergence of the intrinsic thermal conductivity *K* with the system size
- → Thermal conductivity remains finite and does not depend on the system size in 3D

Divergence of the Lattice Thermal Conductivity in 2D and 1D Crystal Lattices

The intrinsic thermal conductivity of 2-D or 1-D anharmonic crystals is anomalous.

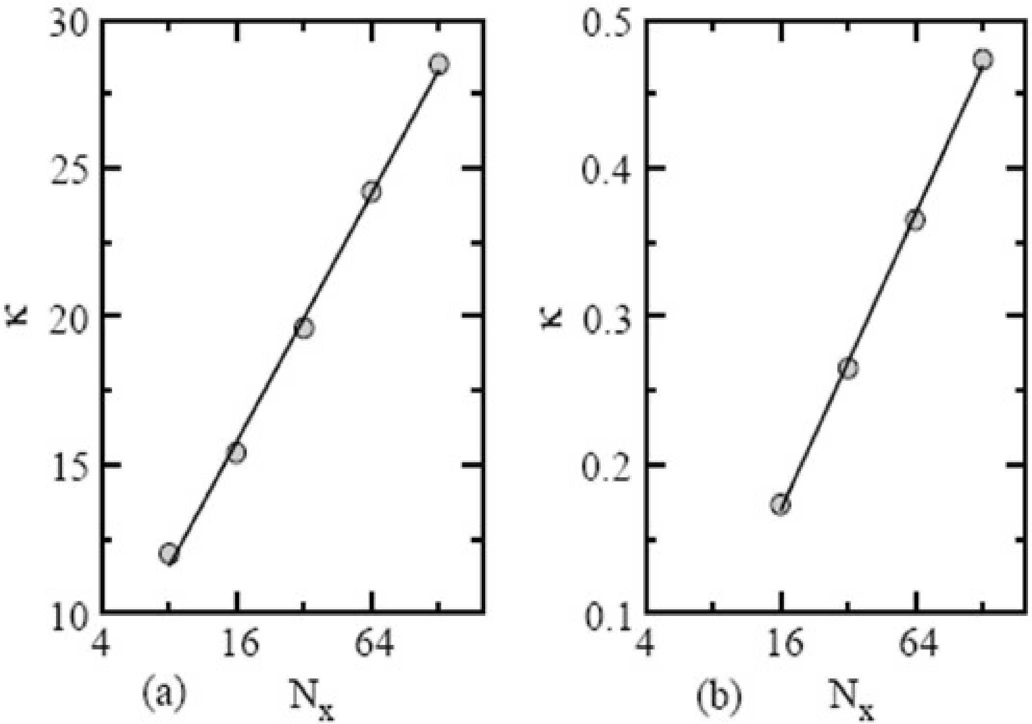

Thermal conductivity in 2D lattice vs. N_x.
Data is after S. Lepri et al. Phys. Rep., 377, 1 (2003).

K ~ log(N) in 2D

K ~ N^{α} in 1D, $\alpha \neq 1$

N – system size

[1] K. Saito, et al., *Phys. Rev. Lett.* (2010).
[2] A. Dhar. *Advances in Physics* (2008).
[3] G. Basile et al. *Eur. Phys. J.* (2007).
[4] L. Yang et al. *Phys. Rev. E* (2006).
[5] L. Delfini et al. *Phys, Rev. E* (2006).
[6] S. Lepri et al. *Chaos* (2005).
[7] J. Wang et al., *Phys. Rev. Lett*. (2004).
[8] S. Lepri et al. *Phys. Rep.* (2003).
[9] R. Livi and S. Lepri. *Nature* (2003).
[10] O. Narayan et al., *Phys. Rev. Lett*. (2002).
[11] A. Dhar. *Phys. Rev. Lett*. (2001).
[12] A. Lepri and R. Livi, *J. Stat. Phys*. (2000).
[13] T. Pozen et al., Phys. Rev. Lett. (2000).
[14] S. Lepri et. al. *Europhys. Lett*. (1998).

Measurement of Thermal Conductivity: Steady-State *vs.* Transient Techniques

Measurement Principles

$$\frac{\dot{Q}}{S} = -K \nabla T$$

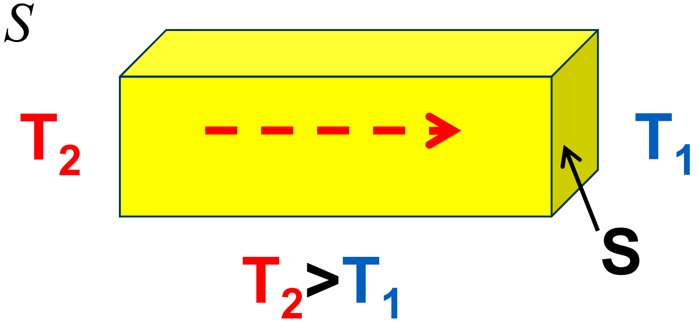

Transient Plane Source Technique

3-ω Thermal Conductivity Setup

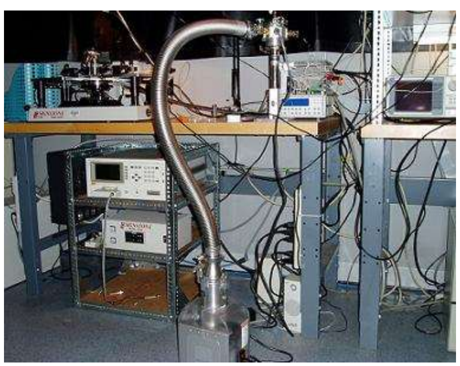

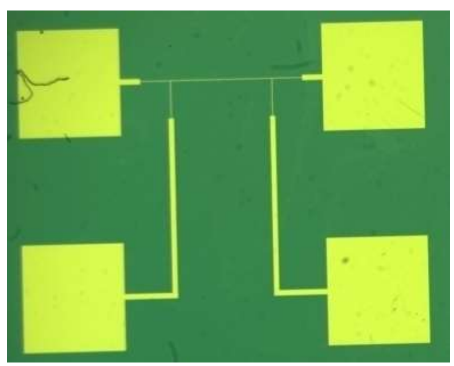

Laser – Flash Technique

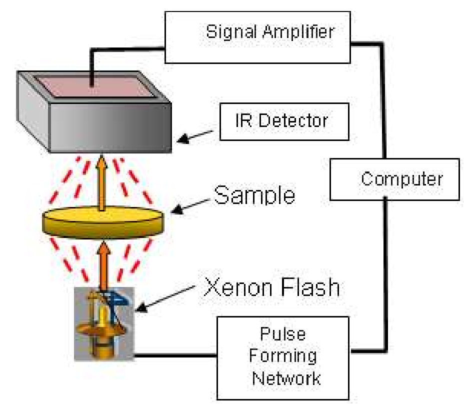

Optical Phonons in Graphene: Raman Spectroscopy

Visualization on Si/SiO_2 substrates

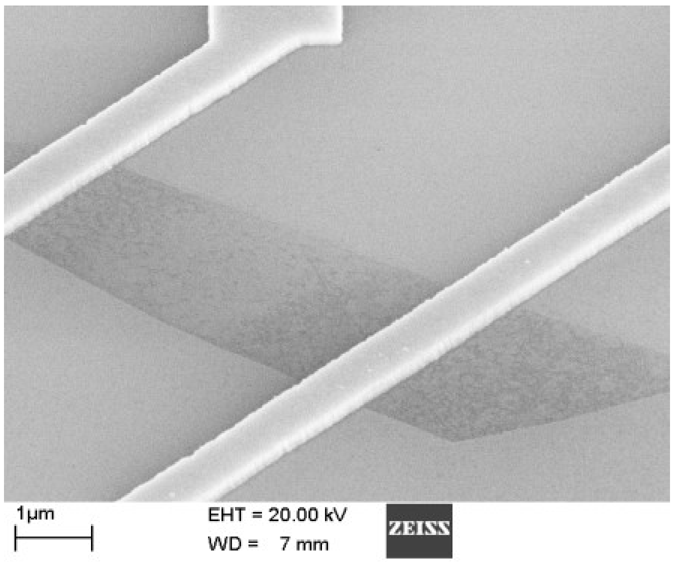

Other techniques:

→ low-temperature transport study

→ cross-sectional TEM

→ few other costly methods

D band: A_{1g} (~1350 cm^{-1}); ***G peak:*** E_{2g}; ***2D* band**

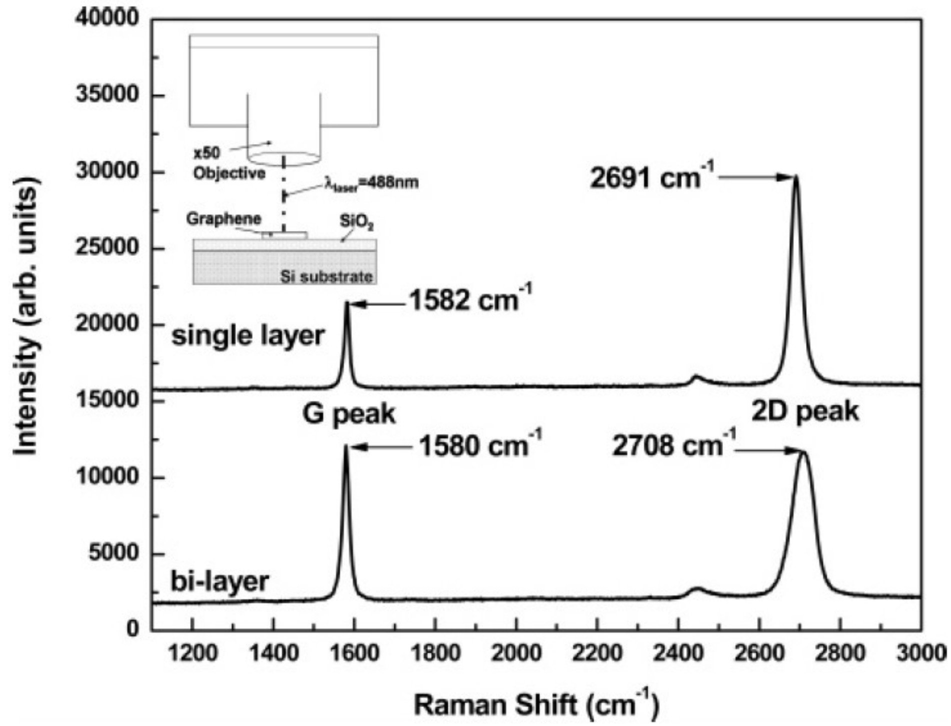

A.C. Ferrari et al., *Phys. Rev. Lett*. **97**, 187401 (2006).

I. Calizo, et al., *Nano Lett.*, **7**, 2645 (2007).

Temperature Shift of the Raman G Peak in Graphene

Note: the sign is negative

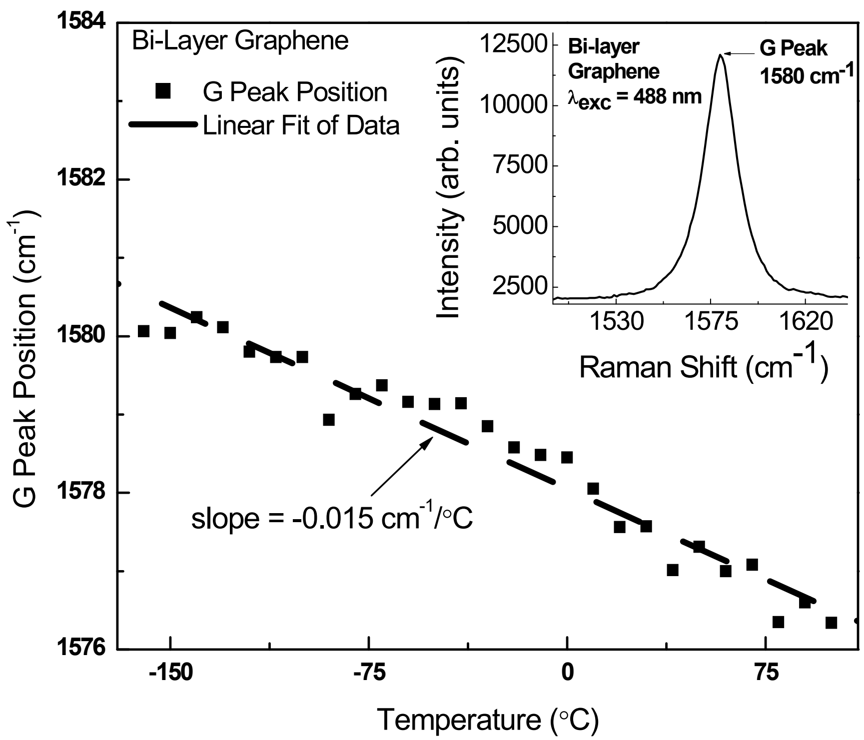

I. Calizo, A.A. Balandin et al., *Nano Lett.*, **7**, 2645 (2007).

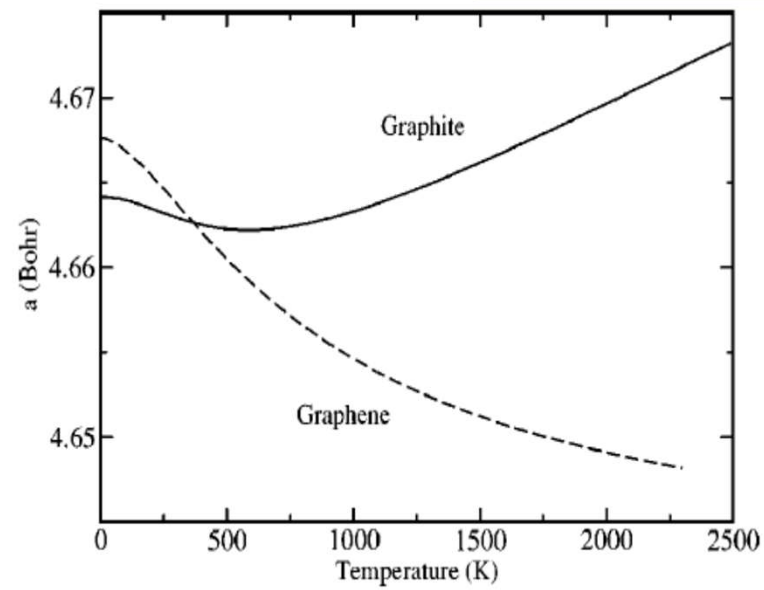

N. Mounet et al, *Phys. Rev. B* **71**, 205214 (2005).

Lifshits Membrane Effect:

И.М. Лифшиц, Журнал Экспериментальной и Теоретической Физики (1952)

Phonon frequency downshift with temperature is unusual when the bond-bond distances shorten with temperature since normally lattice contraction leads to the upward shift of the frequencies.

Temperature Effects on the Phonon Frequencies in Graphene

Comparison of Theory and Experiment

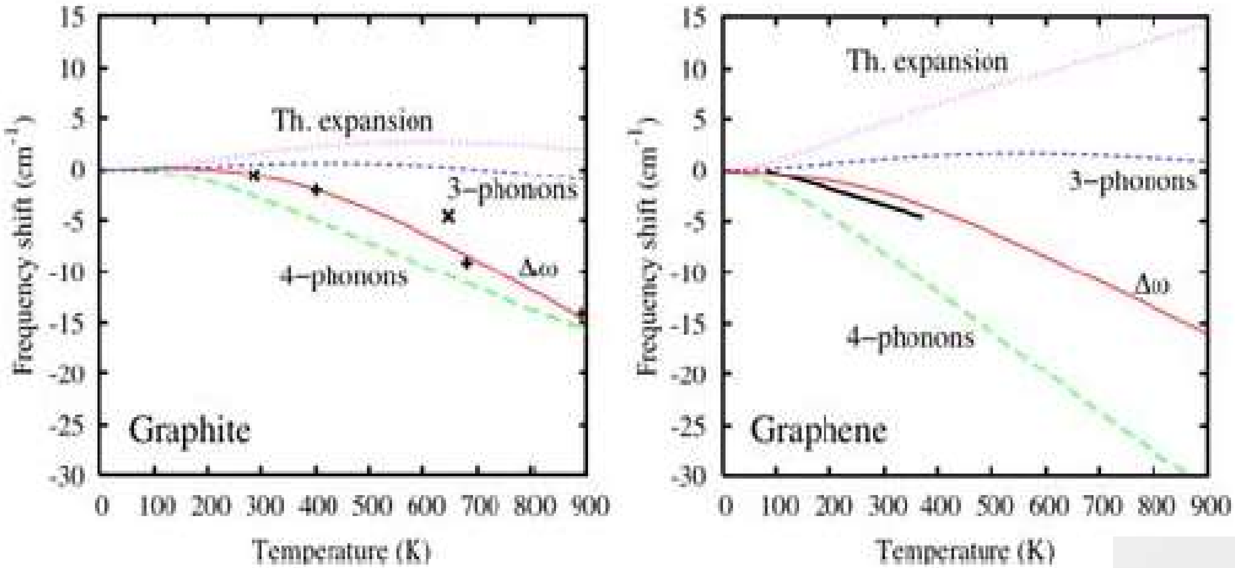

N. Bonini et al., *Phys. Rev. Lett.*, **99**, 176802 (2007).
N. Bonini et al., *phys. stat. sol. (b)*, **245**, 2149 (2008)

Computational data:
Prof. Nicola Marzari, MIT

Raman spectrometer as thermometer

Optothermal technique for measuring thermal conductivity →

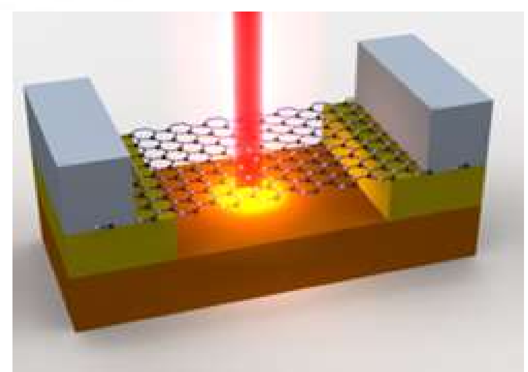

Optothermal Measurement of Graphene Thermal Conductivity

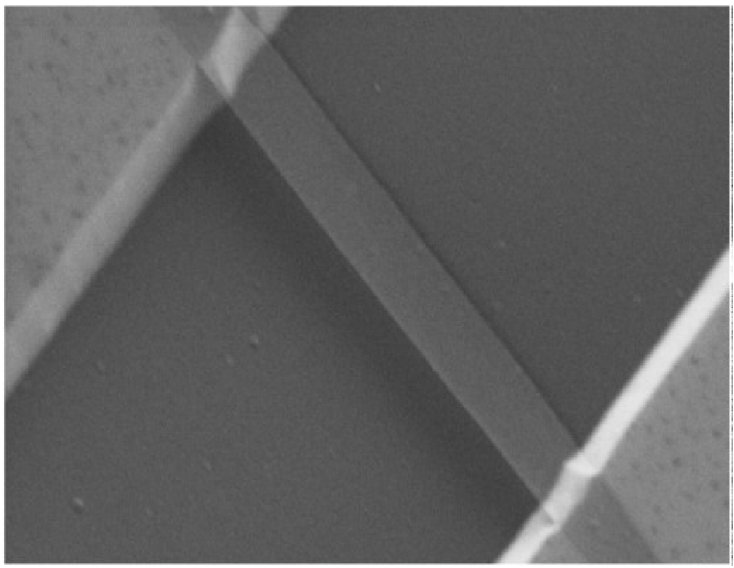

Bilayer graphene ribbon bridging 3-μm trench in Si/SiO_2 wafer

$$K = (L / 2a_G W)\chi_G(\Delta\omega / \Delta P_G)^{-1}.$$

Connect ΔP_D ← → ΔP_G through calibration

→ Laser acts as a heater: ΔP_G

→ Raman "thermometer": $\Delta T_G = \Delta\omega / \chi_G$

→ Thermal conductivity: $K=(L/2a_G W)(\Delta P_G/\Delta T_G)$

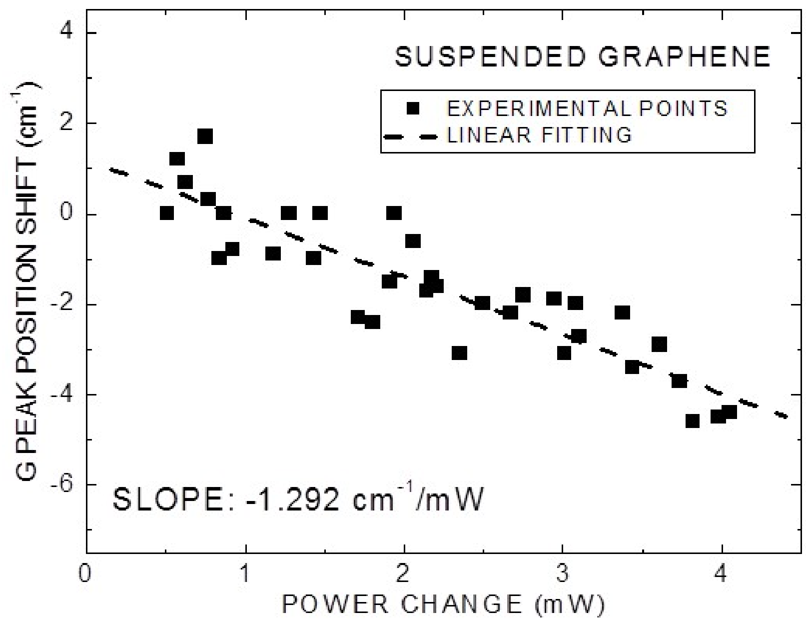

A.A. Balandin, et al., *Nano Letters*, **8**, 902 (2008).

Thermal Conductivity of Graphene: Comparison with CNTs and Theory

Sample	*K (W/mK) near RT*	*Method*	*Comments*	*Refs*
MW-CNT	>3000	electrical self-heating	individual; diffusive	10
SW-CNT	~3500	electrical self-heating	individual; boundary	11
SW-CNTs	1750 - 5800	thermocouples	bundles; diffusive	63
SW-CNT	3000 - 7000	thermocouples	individual; ballistic	64
CNT	1500 - 2900	electrical	individual	65
CNT	~6600	Theory: MD	$K_{CNT} < K_{graphene}$	66
CNT	~3000	Theory: MD	strong defect dependence	67
SW-CNT	~2500	Theory: BTE	$K_{CNT} < K_{graphene}$	69
graphene	~2000 - 5000	Raman optothermal	suspended; exfoliated	UCR
FLG	~1300 - 2800	Raman optothermal	suspended; exfoliated; *n*=4-2	UCR
graphene	~2500	Raman optothermal	suspended; CVD	UTA
graphene	1500 - 5000	Raman optothermal	suspended; CVD	Purdue
graphene	600	Raman optothermal	suspended; exfoliated; T~660 K	CNRS
FLG ribbon	1100	electrical self-heating	supported; exfoliated; *n*<5	GIT
graphene	600	electrical	supported; exfoliated	UTA
graphene	2000 - 5000	Theory: VFF, BTE, $\gamma(q)$	strong width dependence	79
graphene	1 - 5000	Theory: RTA, γ_{TA}, γ_{LA}	strong size dependence	62
graphene	8000 - 10000	Theory: MD, Tersoff	square graphene sheet	80
graphene	1400 - 3400	Theory: BTE	length dependence	69
graphene	~4000	Theory: ballistic	strong width dependence	82

Theory of the Phonon Heat Conduction Graphene

Scattering processes included into consideration:

$$\frac{1}{\tau_{tot}(s,q)} = \frac{1}{\tau_U(s,q)} + \frac{1}{\tau_B(s,q)} + \frac{1}{\tau_{Pd}(s,q)}.$$

Point Defect Scattering

$$\frac{1}{\tau_{PD}(s,q)} = \frac{S_0\Gamma}{4}\frac{q_s(\omega_s)}{v_s(\omega_s)}\omega_s^2,$$

$$\Gamma = \sum_i f_i (1 - M_i / \bar{M})^2$$

Umklapp Scattering:

Phonon-mode dependent Gruneisen parameter from N. Mounet and N. Marzari, Phys. Rev. B, 71, 205214 (2005).

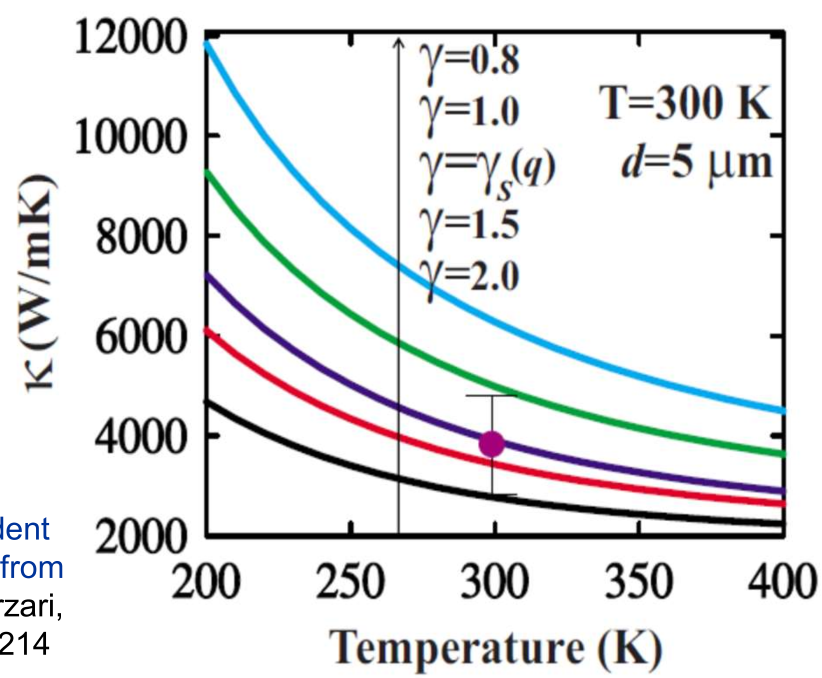

D.L. Nika, E.P. Pokatilov, A.S. Askerov and A.A. Balandin, "Phonon thermal conduction in graphene: Role of Umklapp and edge roughness scattering," Physical Review B 79, 155413 (2009) - Editors' Selection

Theory of Heat Conduction in Graphite and Graphene

Theory of the A-Plane Thermal Conductivity of Graphite
P. G. Klemens
Journal of Wide Bandgap Materials 2000; 7; 332
DOI: 10.1106/7FP2-QBLN-TJPA-NC66

GRAPHENE

Similar considerations also apply to a single graphene sheet. Here the phonon gas is two-dimensional down to zero frequency, since there are no wave vectors outside the basal plane. However, a logarithmic divergence is also prevented, because the mean free path cannot exceed a linear dimension L, determined by the size and shape of the sheet. The factor $C(f)l(f)$ now increases with decreasing frequency only when $f > f_B$, where f_B is given by the condition that $l_i(f_B) = L$. Using Equation (3) this yields

$$f_B^2 = \frac{1}{4\pi\gamma^2}\frac{Mv^2}{kT}\frac{vf_m}{L} \tag{21}$$

Klemens Model of Heat Conduction: Bulk Graphite vs. Graphene

Phonon Thermal Conductivity:

$$K_p = \Sigma_j \int C_j(\omega) \upsilon_j^2(\omega) \tau_j(\omega) d\omega$$

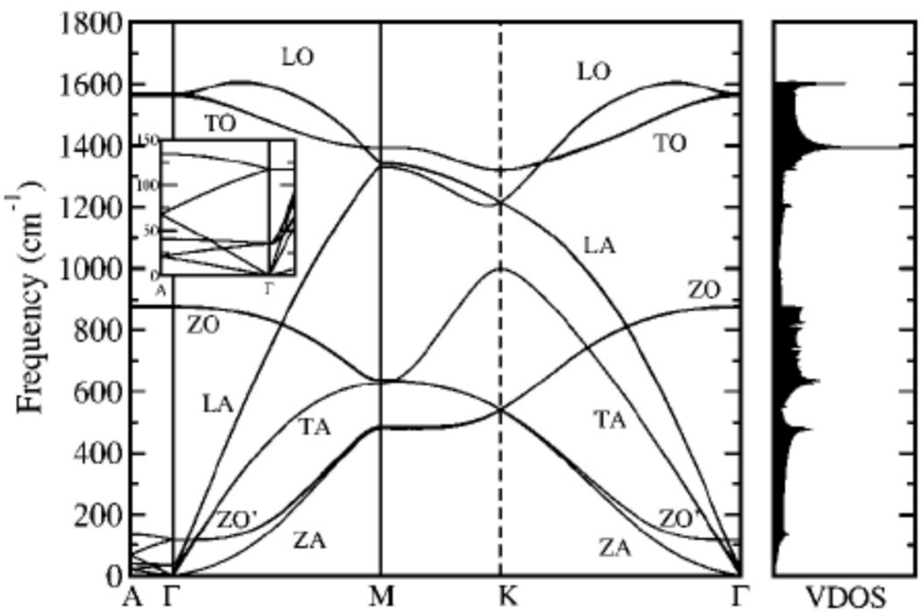

P.G. Klemens, *J. Wide Bandgap Materials*, **7**, 332 (2000).

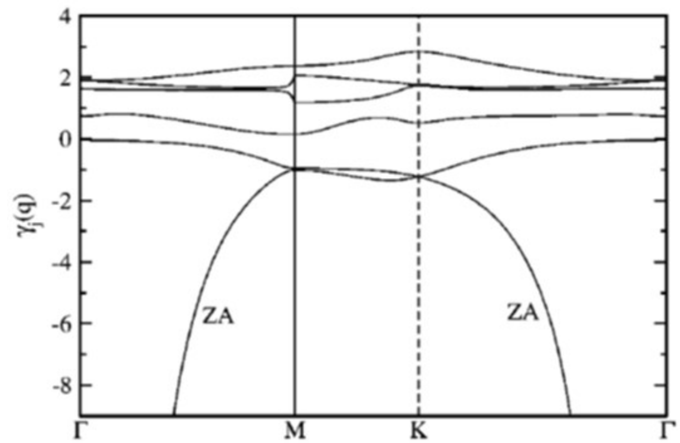

N. Mounet et al, *Phys. Rev. B* **71**, 205214 (2005).

Umklapp life-time, which defines MFP:

$$\tau_{U,s} = \frac{1}{\gamma_s^2} \frac{M \upsilon_s^2}{k_B T} \frac{\omega_{s,\max}}{\omega^2}$$

2D: C(ω) ~ ω → K ~$T^{-1}\omega^{-1}$

3D: C(ω) ~ ω^2

The Role of the Long-Wavelength Phonons in Heat Transport in Graphene

Thermal conductivity in graphene:

$$K \propto \frac{1}{\omega_m} \int_{\omega_C}^{\omega_m} \frac{d\omega}{\omega} \propto \frac{1}{\omega_m} \ln\left(\frac{\omega_m}{\omega_C}\right).$$

Graphene:

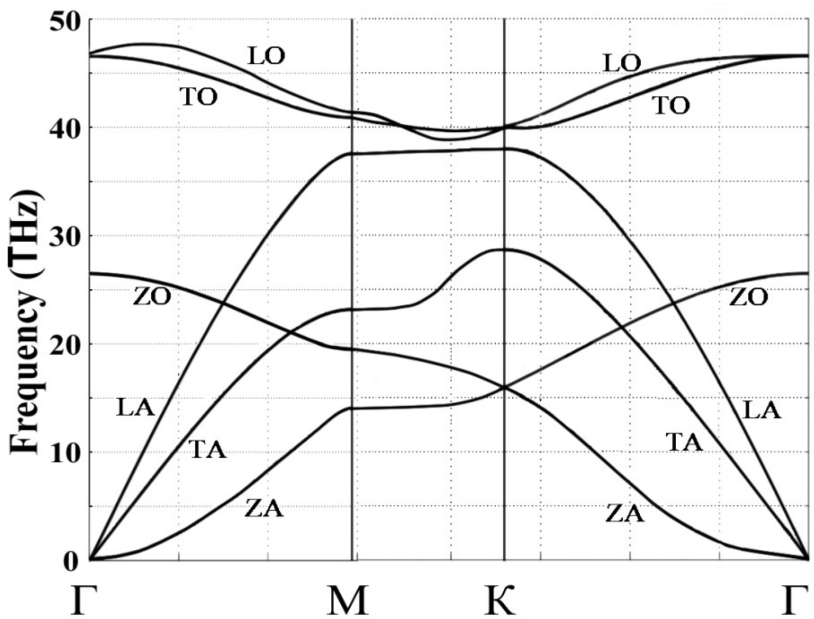

MFP = L – physical size of the system

→ Limitation on MFL: $L=\tau v_s$

$$\tau_{U,s} = \frac{1}{\gamma_s^2} \frac{M \upsilon_s^2}{k_B T} \frac{\omega_{s,\max}}{\omega^2}$$

→ Limiting low-bound frequency:

$$\omega_{s,\min} = \frac{\upsilon_s}{\gamma_s} \sqrt{\frac{M \upsilon_s}{k_B T} \frac{\omega_{s,\max}}{L}}$$

$$K = (2\pi\gamma^2)^{-1} \rho(\upsilon^4 / f_m T) \ln(f_m / f_B),$$

$$f_B = \left(M\upsilon^3 f_m / 4\pi\gamma^2 k_B T L\right)^{1/2}$$

Uniqueness of Heat Conduction in Graphene

Breakdown of Fourier's Law vs. Size-Dependent Intrinsic Thermal Conductivity

The phonon transport in graphene is 2D all the way down to zero frequency

Low-bound cut-off frequency is defined by the condition that the phonon MFP can not exceed the physical size of the graphene flake:

$$\omega_{s,\min} = \frac{\upsilon_s}{\gamma_s}\sqrt{\frac{M\upsilon_s}{k_B T}\frac{\omega_{s,\max}}{L}}$$

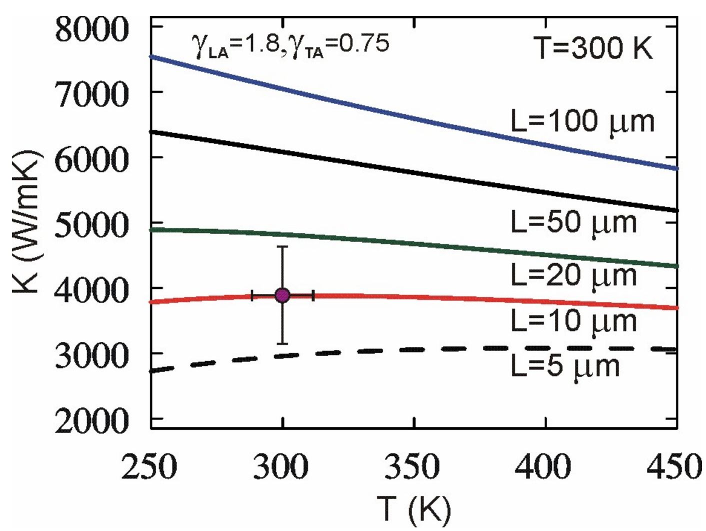

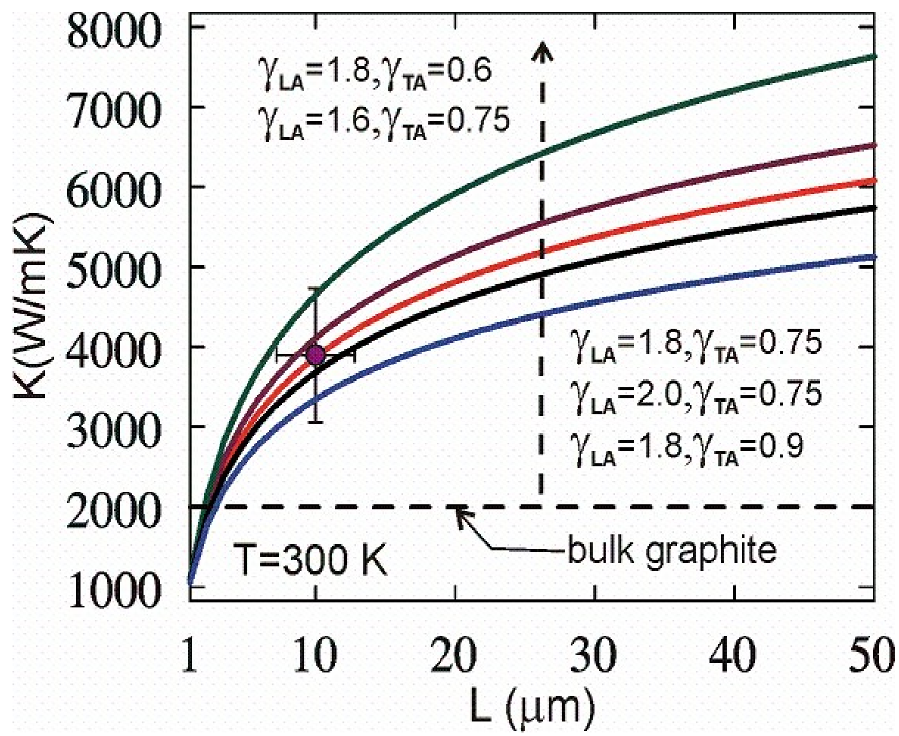

D.L. Nika, S. Ghosh, E.P. Pokatilov, A.A. Balandin, *Appl. Phys. Lett.*, **94**, 203103 (2009).

Evolution of the Intrinsic Thermal Conductivity in Low-Dimensional Systems

Experiment and Umklapp Scattering Theory

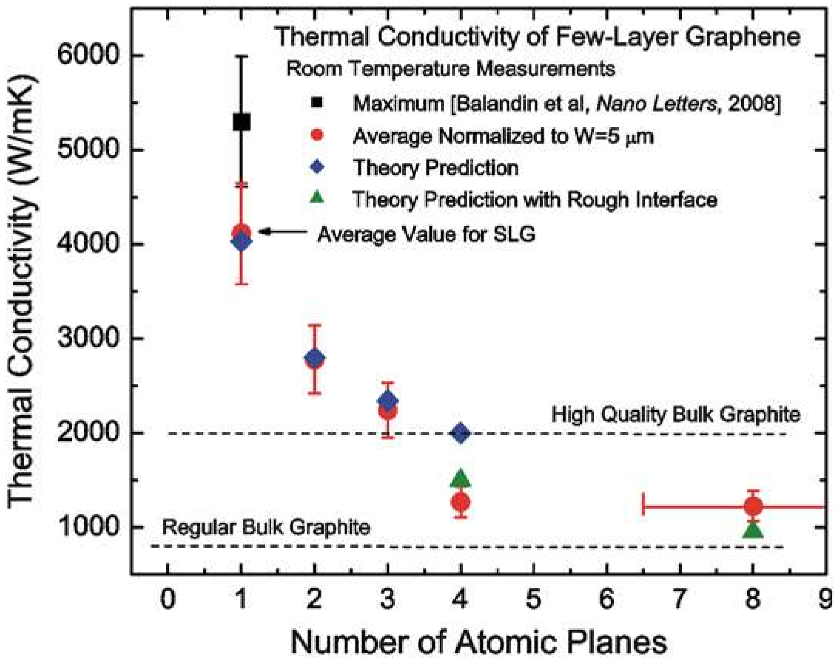

S. Ghosh, W. Bao, D.L. Nika, S. Subrina, E.P. Pokatilov, C.N. Lau and A.A. Balandin, "Dimensional crossover of thermal transport in few-layer graphene," *Nature Materials*, **9**, 555 (2010).

Nonequilibrium Molecular Dynamics Study

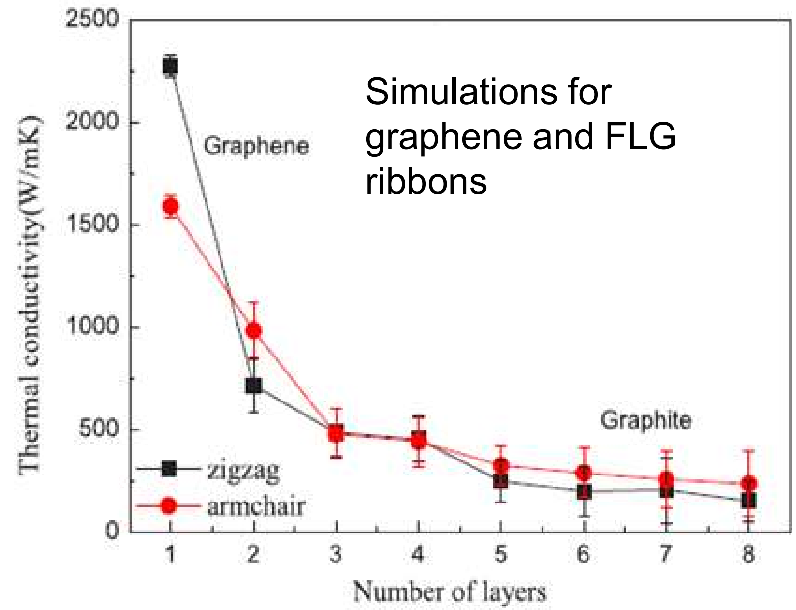

W.-R. Zhong et al., *Appl. Phys. Lett.*, **98**, 113107 (2011).

Consistent with the prediction:

S. Berber,Y.-K. Kwon, and D. Tomanek, *Phys. Rev. Lett.*, **84**, 4613 (2000).

Comparison of Intrinsic Thermal Conductivity in SLG and BLG

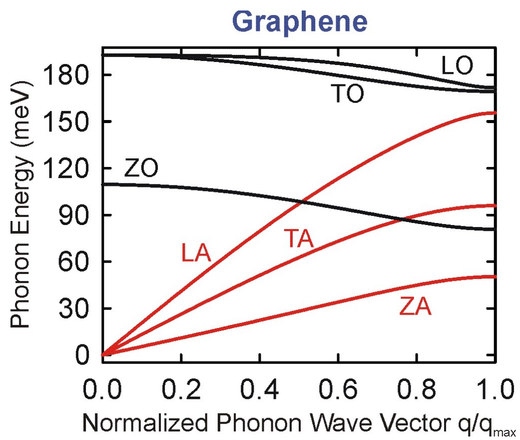

→ In BLG the number of available phonon branches doubles

→ The new conduction channels do not transmit heat effectively in the low-energy regime

→ Phase space available for Umklapp scattering

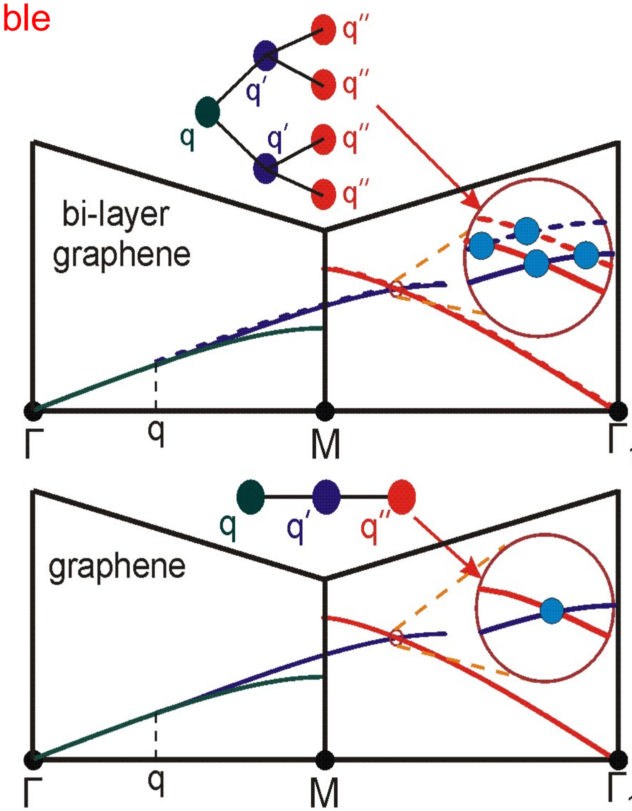

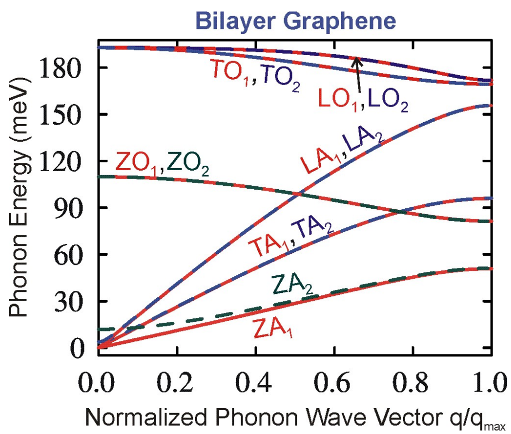

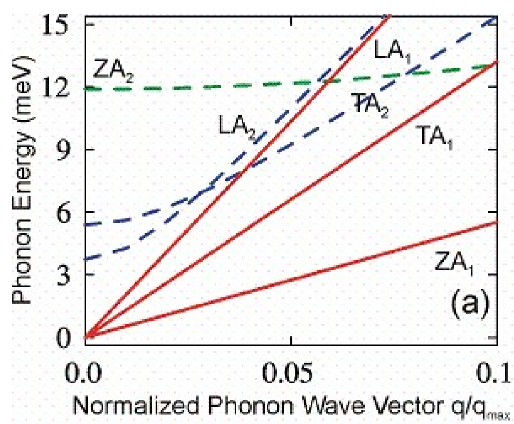

S. Ghosh, W. Bao, D.L. Nika, S. Subrina, E.P. Pokatilov, C.N. Lau and A.A. Balandin, "Dimensional crossover of thermal transport in few-layer graphene," Nature Materials, 9 555 (2010).

Extrinsically Limited Thermal Conductivity of the Encased Graphene and DLC Films

Encased Few-Layer Graphene

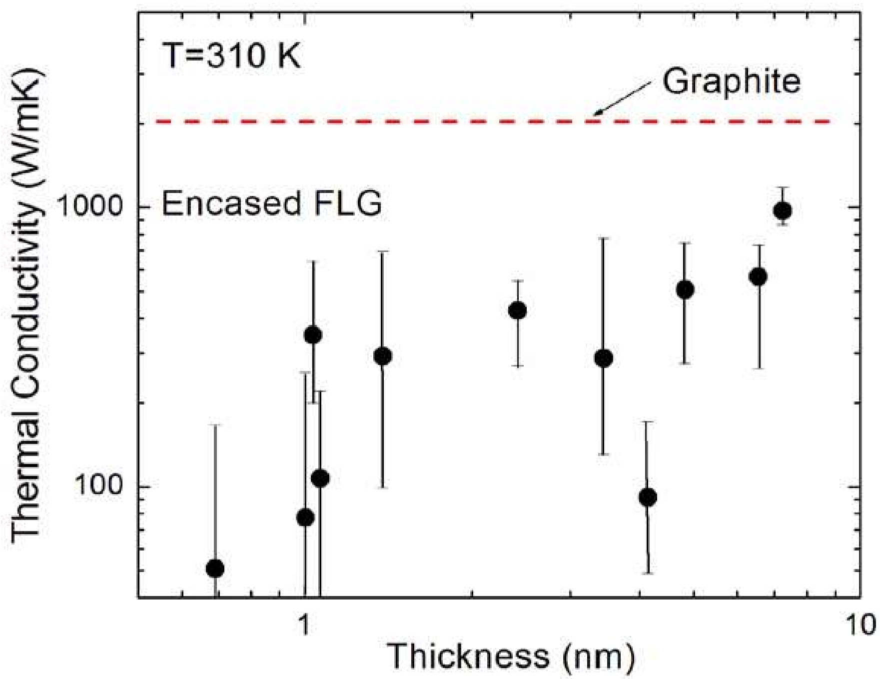

Adapted from Jang, W., Chen, Z., Bao, W., Lau, C.N., and Dames, C., Nano Lett., 10, 3909 (2010).

Encased Diamond-Like Carbon

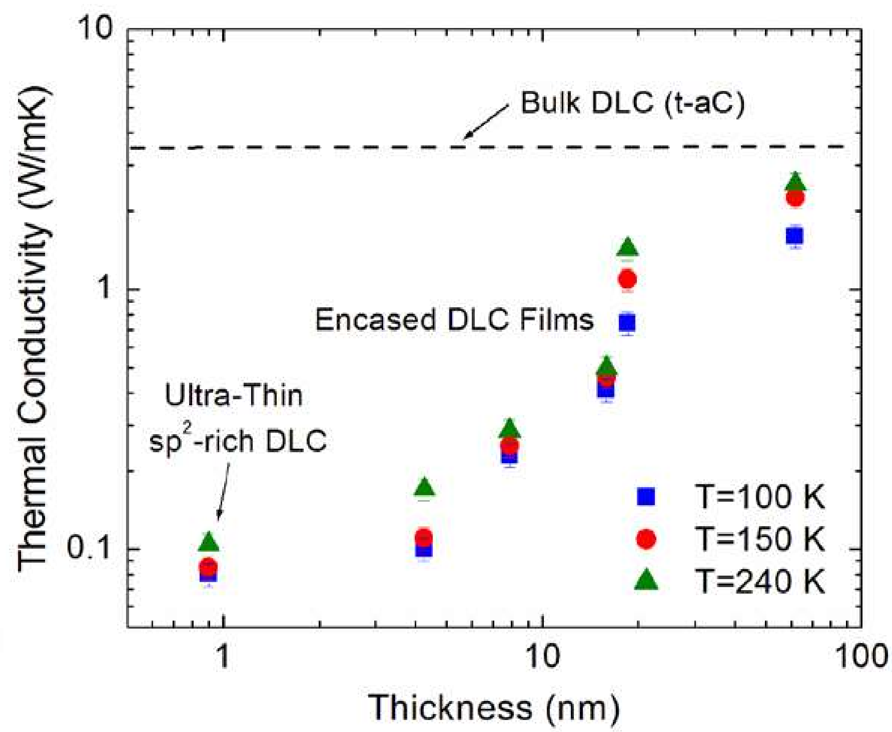

Adapted from Balandin, A.A., Shamsa, M., Liu, W.L., Casiraghi, C., and Ferrari, A.C., Appl. Phys. Lett., 93, 043115 (2008).

Phonons in Isotopically Engineered Graphene

Cooperation with Prof. Rod Ruoff

^{13}C (lower) and ^{12}C (higher) difference: ~ 64 cm^{-1}

$$\omega \propto M^{-1/2}$$

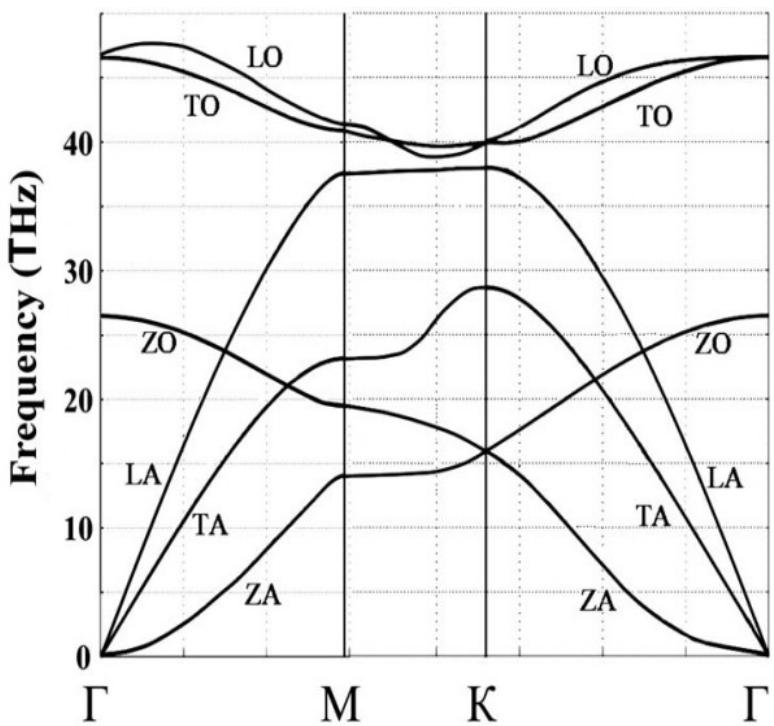

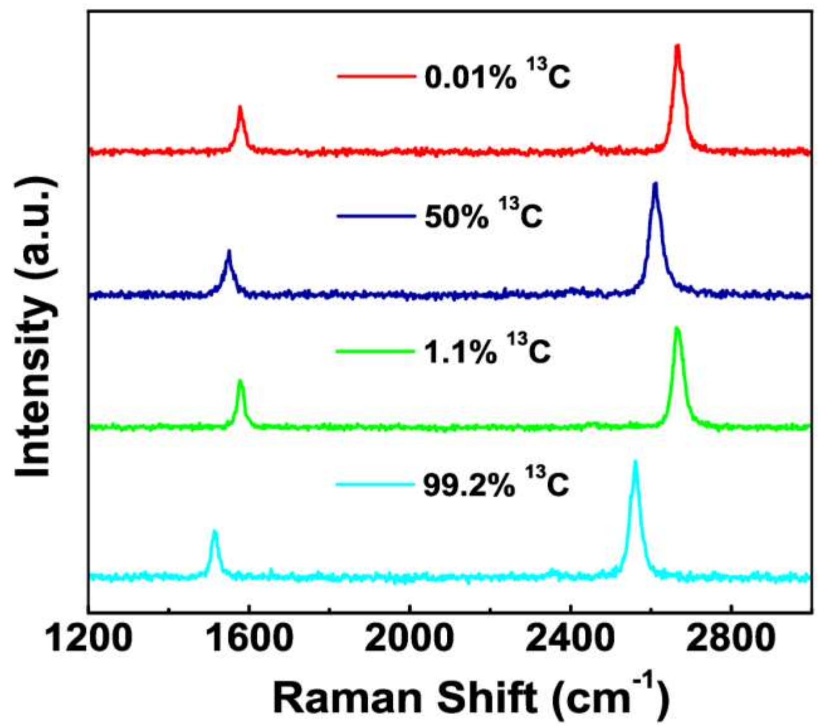

S. Chen, Q. Wu, C. Mishra, J. Kang, H. Zhang, K. Cho, W. Cai, A.A. Balandin and R.S. Ruoff, "Thermal conductivity of isotopically modified graphene," *Nature Materials*, 11, 203 (2012).

Thermal Transport in Isotopically Engineered Graphene

Cooperation with Prof. Rod Ruoff

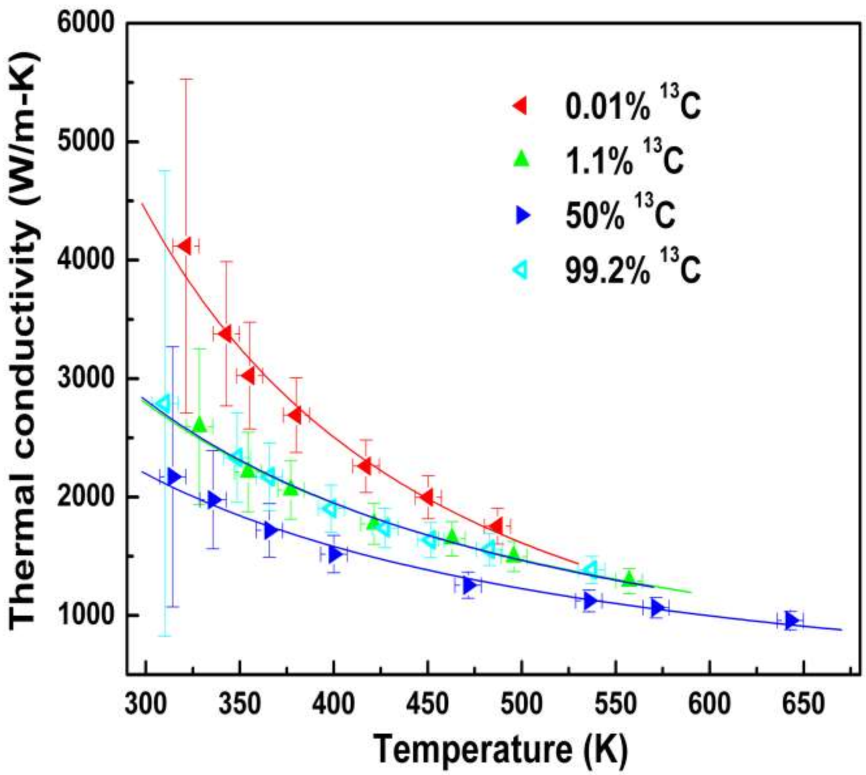

The thermal conductivity, K, of isotopically pure ^{12}C (0.01% ^{13}C) graphene was higher than 4000 W/mK at T~320 K

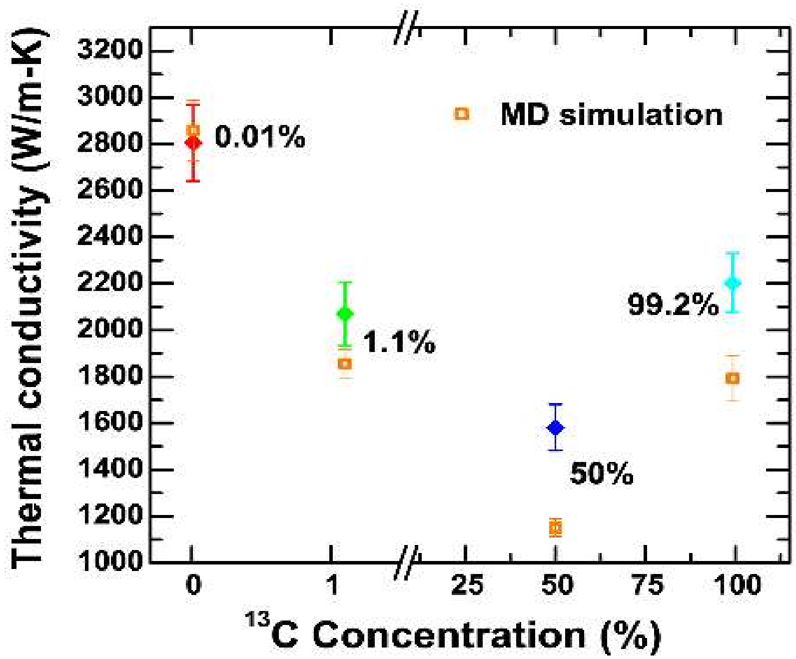

S. Chen, Q. Wu, C. Mishra, J. Kang, H. Zhang, K. Cho, W. Cai, A.A. Balandin and R.S. Ruoff, "Thermal conductivity of isotopically modified graphene," *Nature Materials*, 11, 203 (2012).

Increasing Importance of the Thermal Interface Materials - TIMs

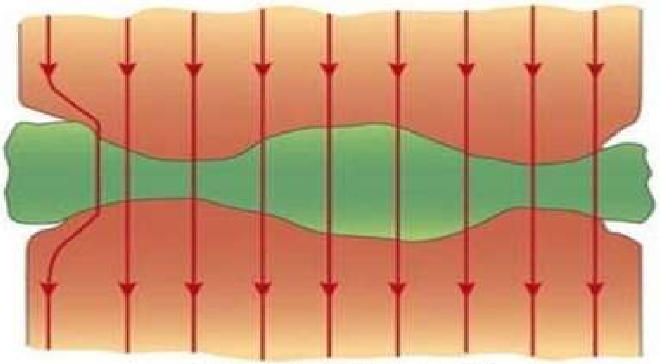

$$R_{effective} = \frac{BLT}{k_{TIM} A} + R_{c_1} + R_{c_2}$$

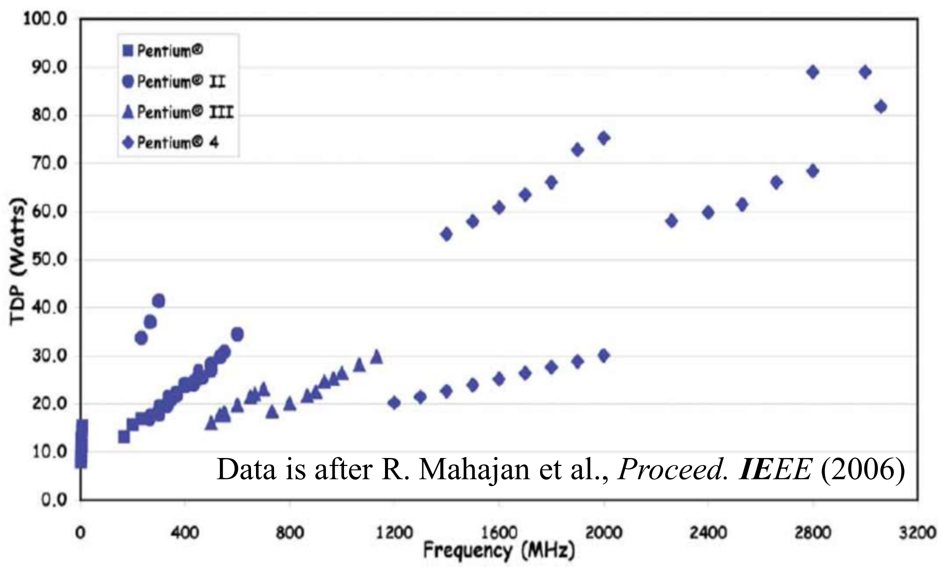

Current TIM based on polymer, grease filled with silver, alumina require 50-70% loading to achieve 1-5 W/mk.

→ Conventional TIMs: K=1-5 W/mK at the volume fractions *f* of filler ~50% at RT

→ Companies need K=25-30 W/mK

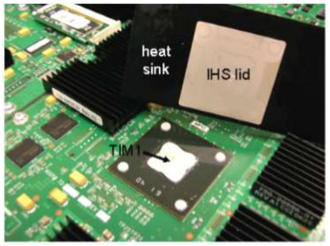

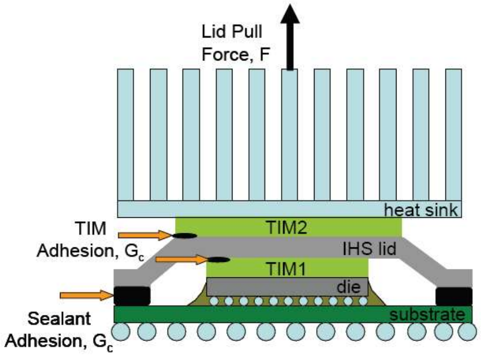

Graphene Enhanced Thermal Interface Materials

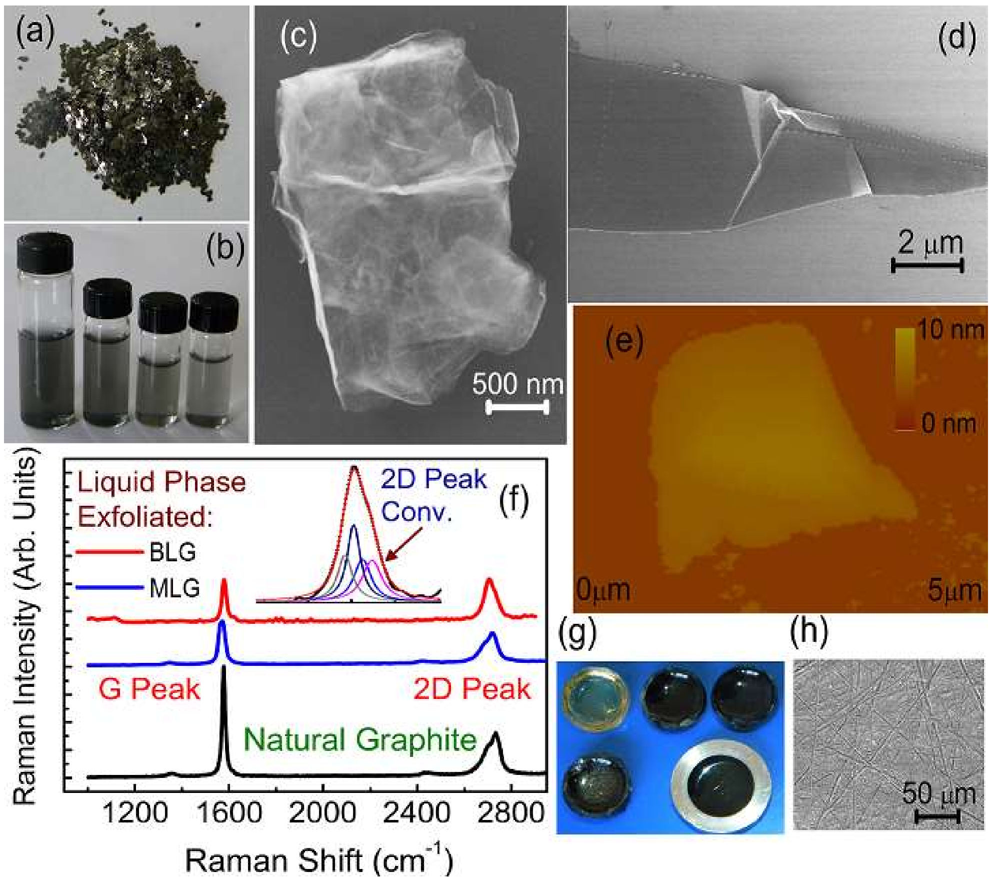

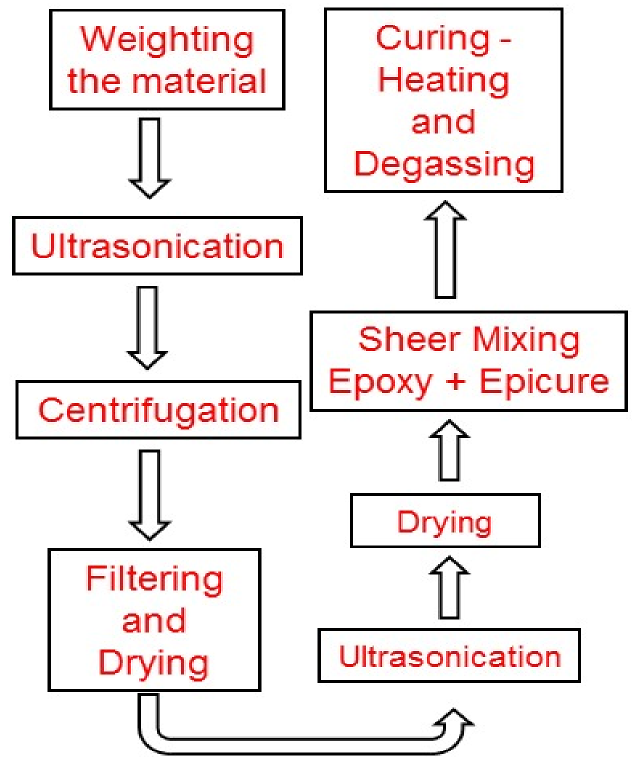

aqueous solution of sodium cholate

K.M.F. Shahil and A.A. Balandin, "Graphene - multilayer graphene nanocomposites as highly efficient thermal interface materials," *Nano Letters*, 12, 861 (2012).

Graphene TIMs with Strongly Enhanced Thermal Conductivity

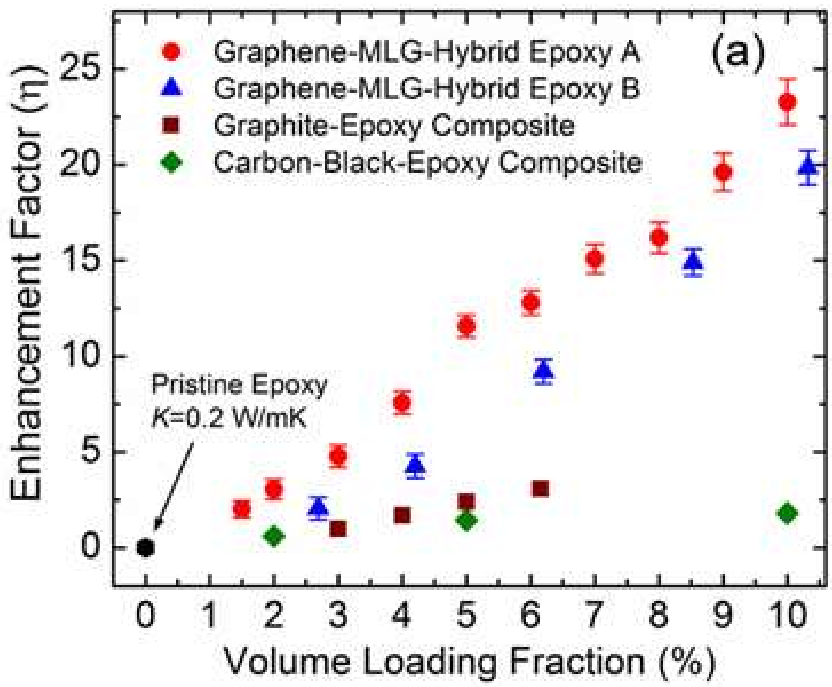

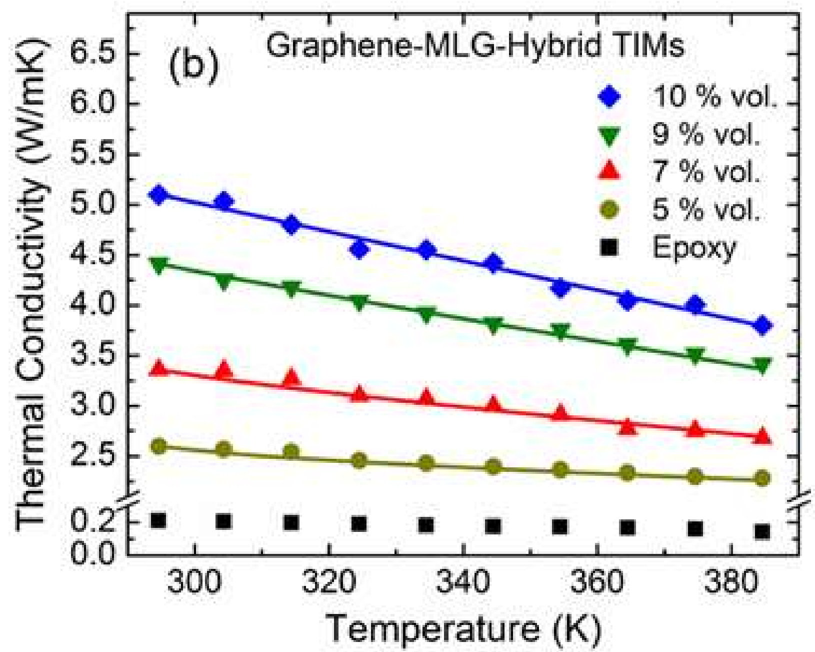

→ Record-high enhancement of *K* by 2300 % in the graphene-polymer at the loading fraction *f* =10 vol.%.

→ K of the commercial thermal grease was increased to K=14 W/mK at the small loading *f*=2 vol. %

K.M.F. Shahil and A.A. Balandin, "Graphene - multilayer graphene nanocomposites as highly efficient thermal interface materials," *Nano Letters*, 12, 861 (2012).

Graphene Composites with Strongly Enhanced Thermal Conductivity

- → Graphene's flexibility and planar geometry improves coupling to the matrix materials
- → Graphene is better than CNTs as fillers owing to its geometry
- → Smaller thermal interface resistance
- → LPE graphene is inexpensive

Next big step:
graphene flake orientation

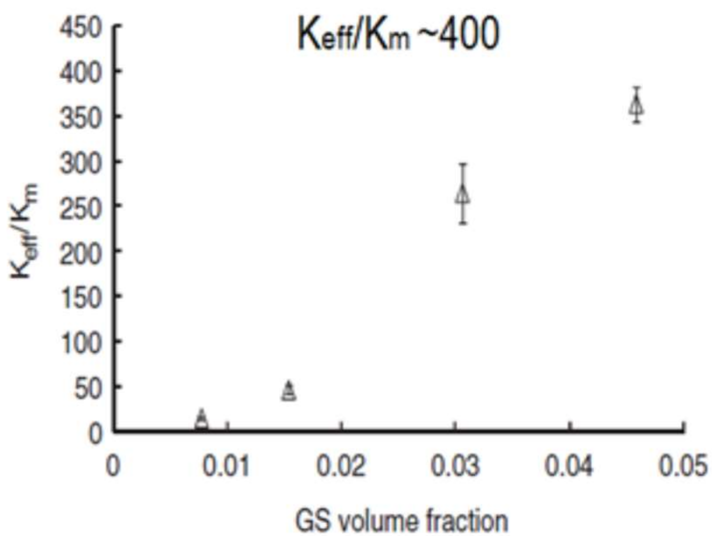

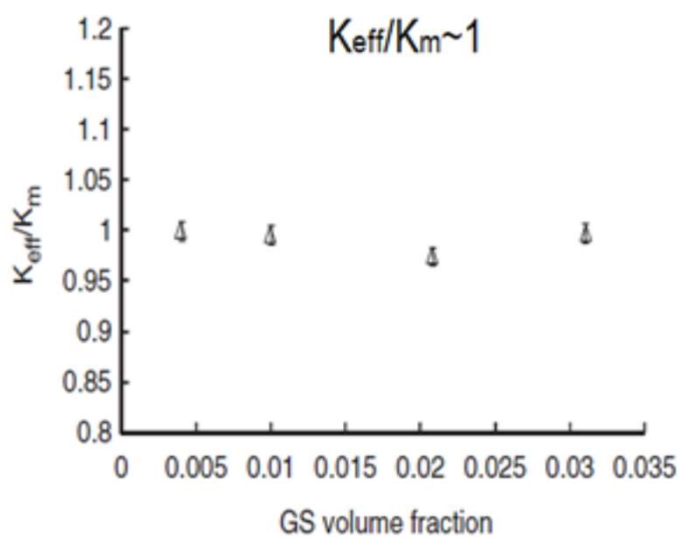

Figure adopted from D. Konatham, K.N.D. Bui, D.V. Papavassiliou and A. Striolo, Simulation insights into thermally conductive graphene-based nanocomposites, Molecular Physics, 109, 97 (2011).

Thermal Phase Change Materials with Graphene

Can graphene make PCM not only to store heat but also to conduct it away?

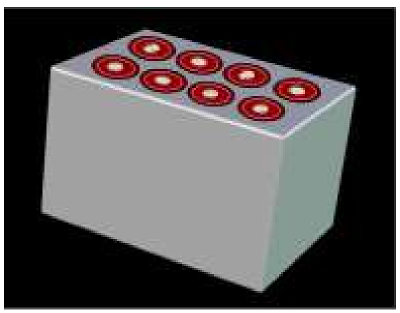

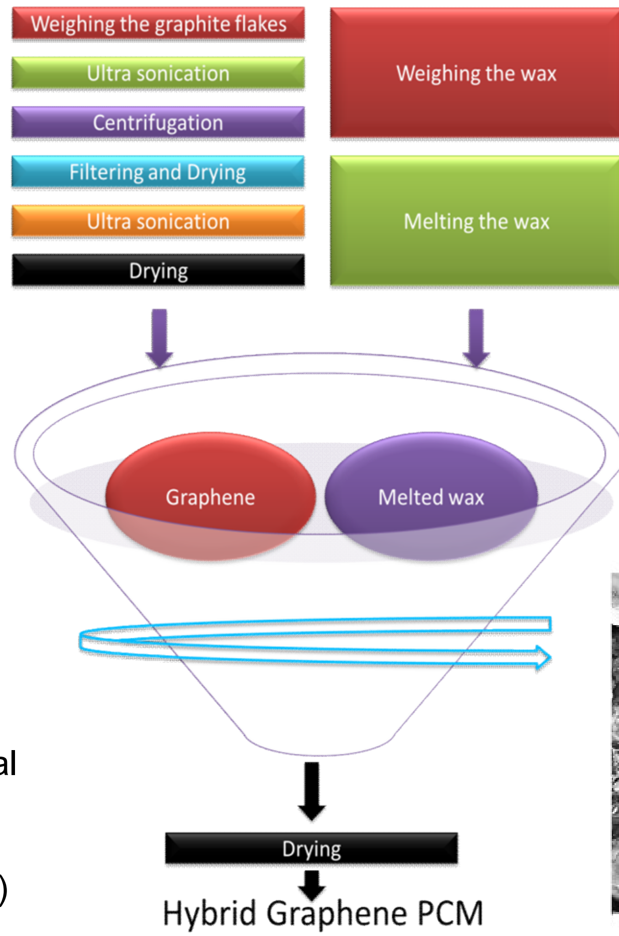

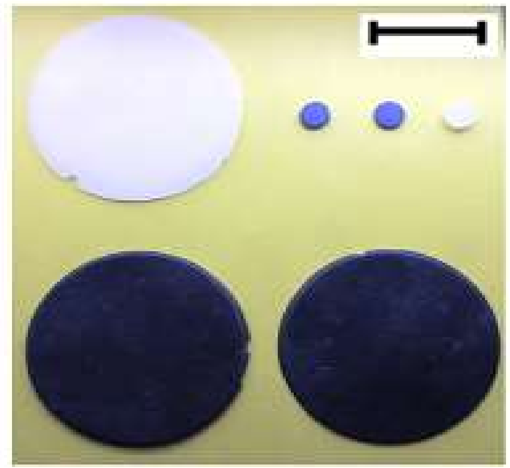

P. Goli, et al., "Graphene-Enhanced Hybrid Phase Change Materials for Thermal Management of Li-Ion Batteries" Journal of Power Sources, 248, 37 – 43 (2014)

Hydrocarbon – Graphene Composites as PCMs with Enhanced Thermal Conductivity

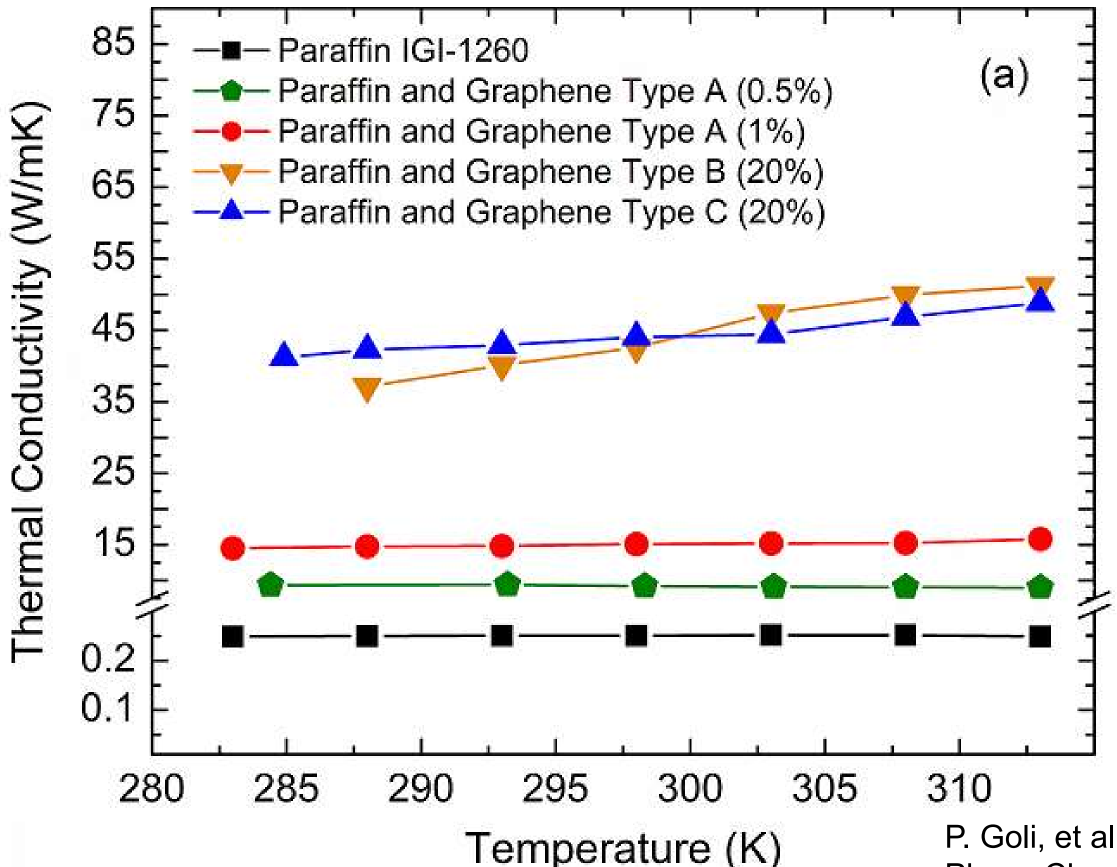

The thermal conductivity enhancement factor, $h=(K-K_m)/K_m$, of about 60 at the 1 wt. % loading fraction is exceptionally high

It is unlikely that uniformly dispersed graphene flakes with a lateral size in the range from 150 to 3000 nm form a thermally percolating network at 1 wt. %

Strongly increased thermal conductivity of the composite is explained by good attachment of hydrocarbon molecules to graphene flakes

P. Goli, et al., "Graphene-Enhanced Hybrid Phase Change Materials for Thermal Management of Li-Ion Batteries" Journal of Power Sources, 248, 37 – 43 (2014)

Testing C_nH_{2n+2} – Graphene Composites for PCM for Battery Thermal Management

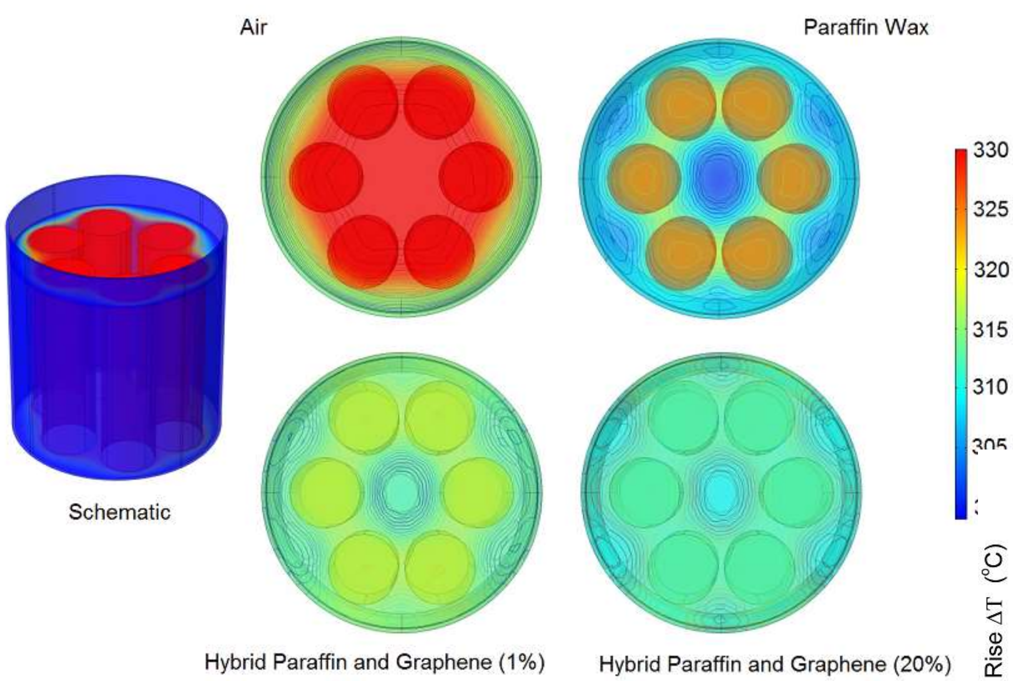

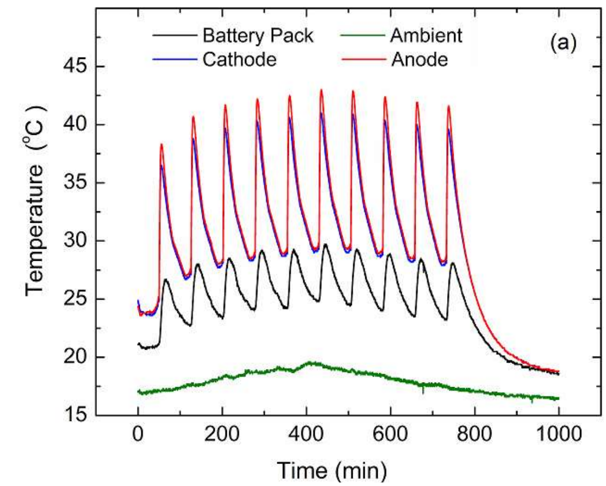

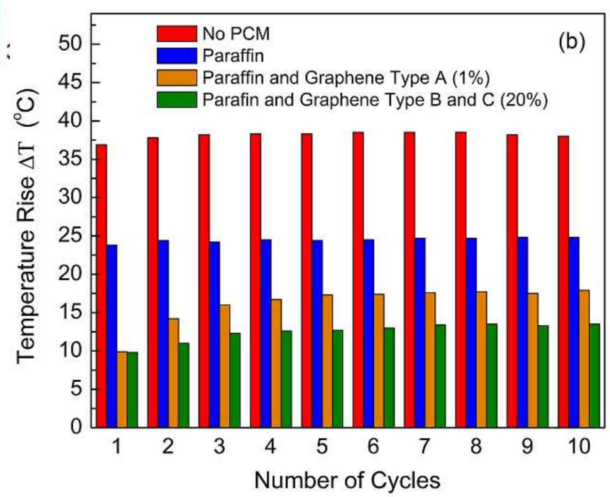

Reduced temperature rise and increased reliability of Li-ion batteries

Graphene *Quilts* for Thermal Management GaN Technology

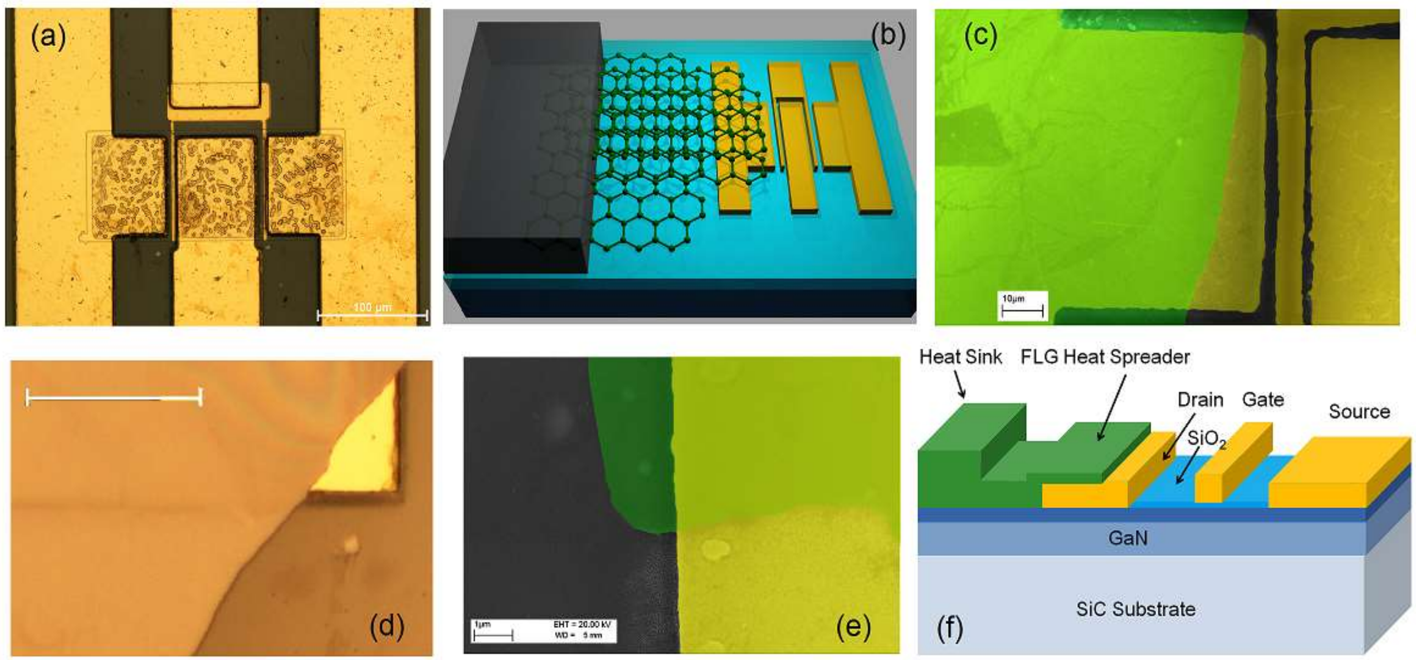

GaN HFETs were used as examples of high-power density transistors; PMMA was utilized as the supporting membrane for graphene transfer to a desired location; the alignment was achieved with the help of a micromanipulator

Z. Yan, G. Liu, J.M. Khan and A.A. Balandin, Graphene-Graphite Quilts for Thermal Management of High-Power Transistors, *Nature Communications* **3**, 827 (2012).

| Nano-Device Laboratory >

Reduction of the Hot-Spot Temperature

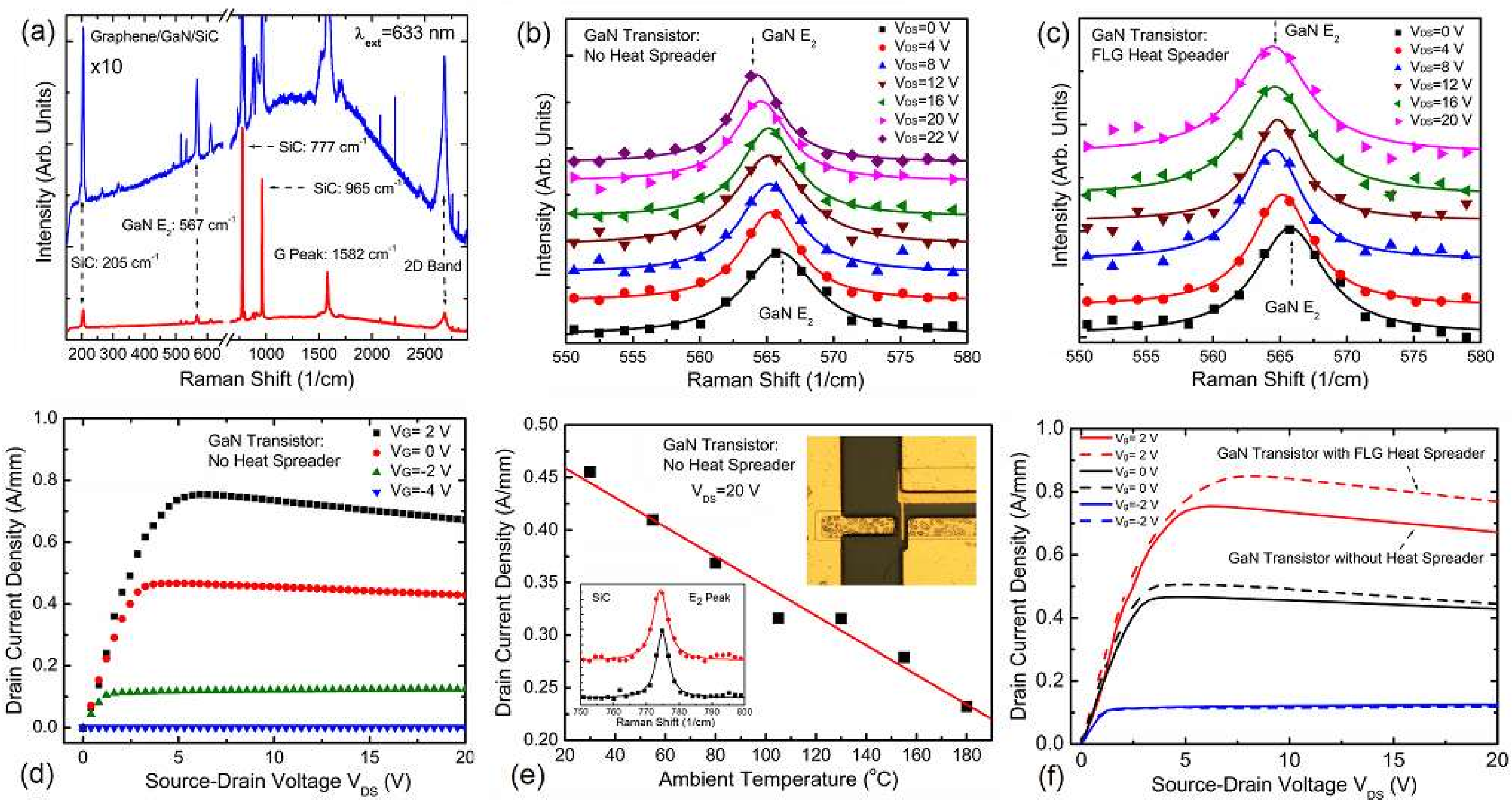

The hot-spots temperature near drain contacts can be lowered by as much as ~ 20°C in such devices operating at ~13-W/mm – translates to an order of magnitude improvement in MTTF

Thermal Properties of Copper Foils Coated with CVD Graphene

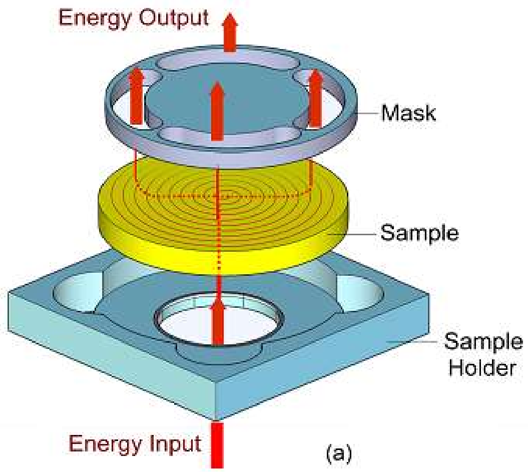

(a)

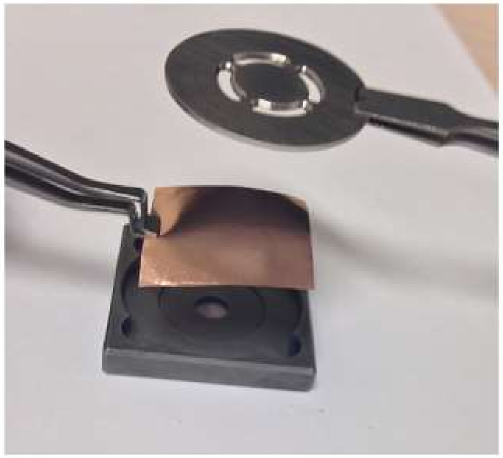
(b)


(c)

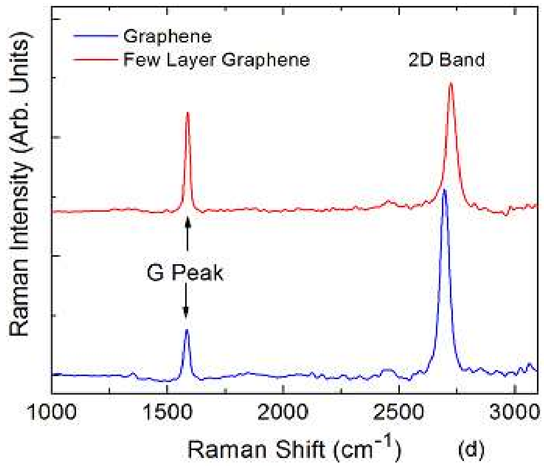

(d)

Cooperation with
Prof. Konstantin Novoselov
and Bluestone Global Tech

(a) Schematic of the modified “laser flash” experimental setup for measuring in-plane thermal diffusivity.
(b) Cu film coated with CVD graphene placed on the sample holder.
(c) Back side of the sample holder with the slits for measuring temperature.
(d) Raman spectrum of graphene and few-layer graphene on Cu. The data is presented after background subtraction.

Thermal Properties of Graphene – Copper – Graphene Hetero-Films

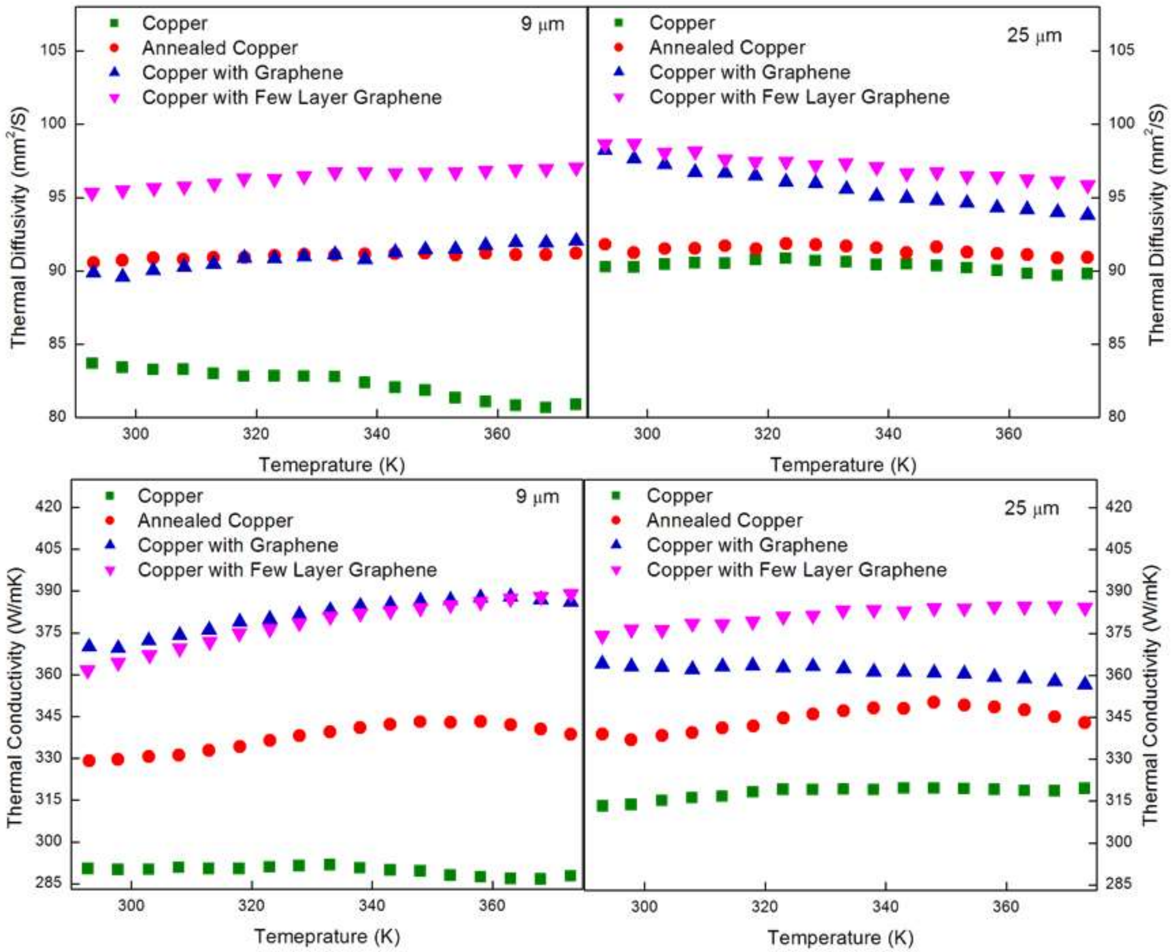

Cooperation with Prof. Konstantin Novoselov and Bluestone Global Tech

→ CVD of graphene on both sides of 9-μm-thick Cu films increases their thermal conductivity by 24% near room temperature.

→ Thermal resistance R=L/(KhW) of the additional heat conduction channel via graphene is much larger than via Cu film.

P. Goli, H. Ning, X. Li, C.Y. Lu, K.S. Novoselov and A.A. Balandin, arXiv:1311.6029 (2013)

| Nano-Device Laboratory >

Enlargement of Cu Grain Size During CVD of Graphene

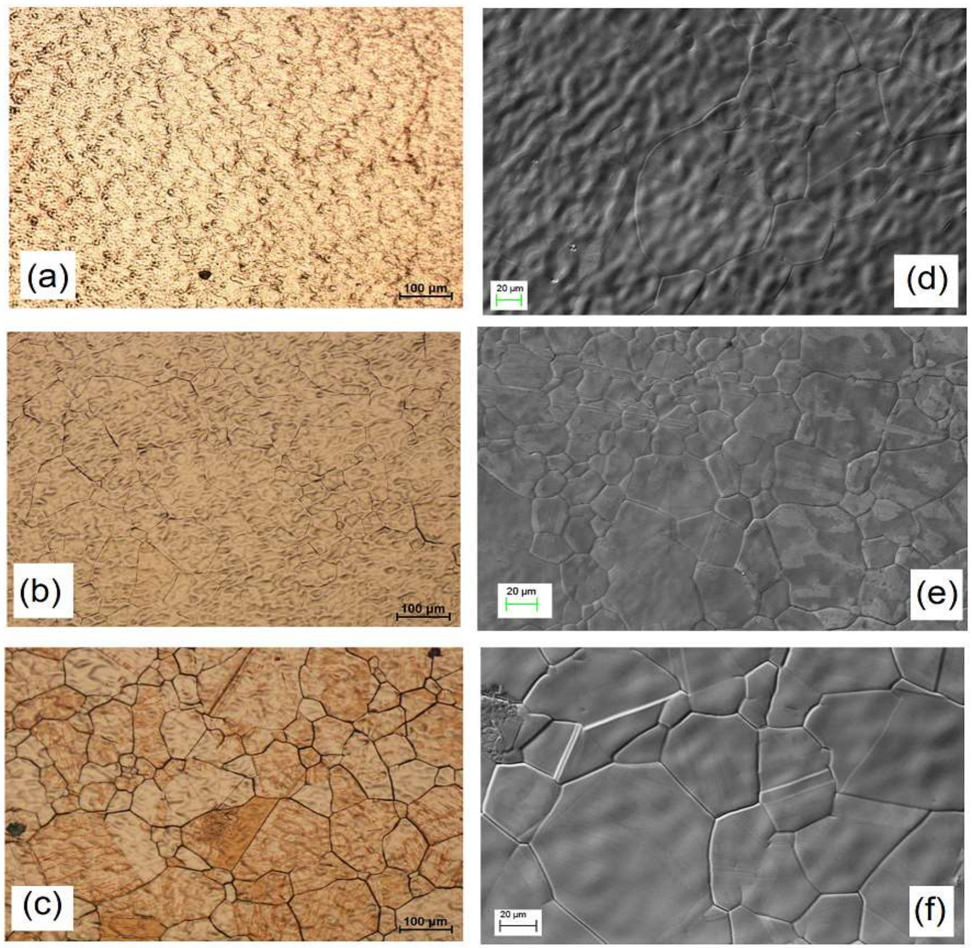

Cooperation with
Prof. Konstantin Novoselov
and Bluestone Global Tech

Thermal conductivity *K* of a polycrystalline metal through that of a single-crystal metal:

$$K = (1 + \Lambda / D)^{-1} K_B$$

$$\frac{\tilde{D}}{D} = \frac{1 - (\Delta K / K)}{1 + (\Delta K / K)(D / \Lambda)}$$

If one assumes that the average grain diameters are in the range D≈1-10 μm, the measured ΔK/K=0.2 can be achieved for if the ratio varies from ~0.13 to 0.016, which corresponds to the grains in reference Cu on the order of 130 – 160 nm.

P. Goli, H. Ning, X. Li, C.Y. Lu, K.S. Novoselov and A.A. Balandin, arXiv:1311.6029 (2013)

| Nano-Device Laboratory >

Graphene-on-Diamond – Carbon-on-Carbon Interconnect Technology

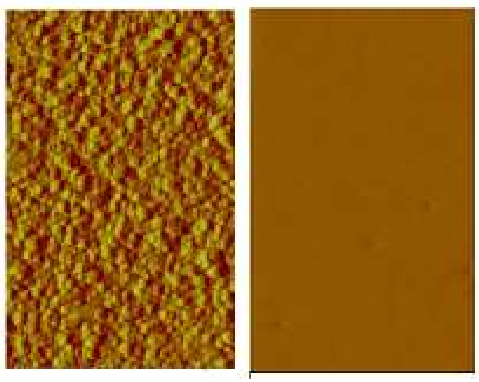

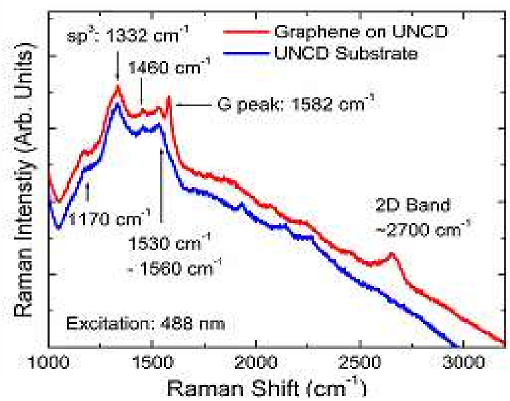

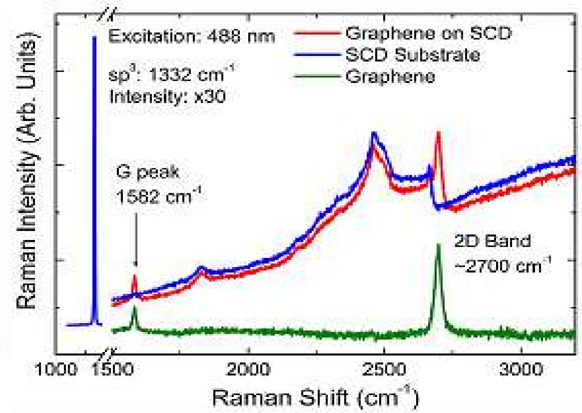

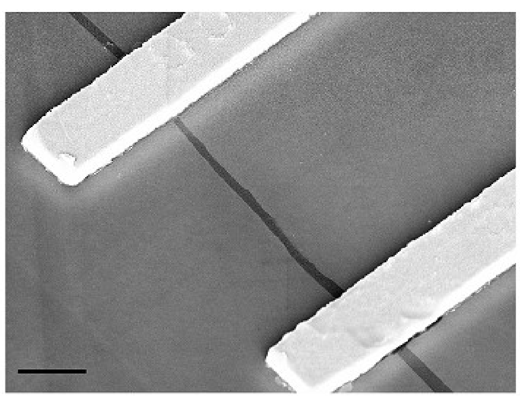

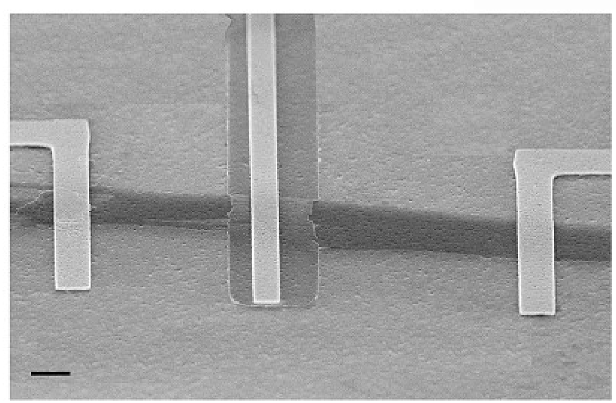

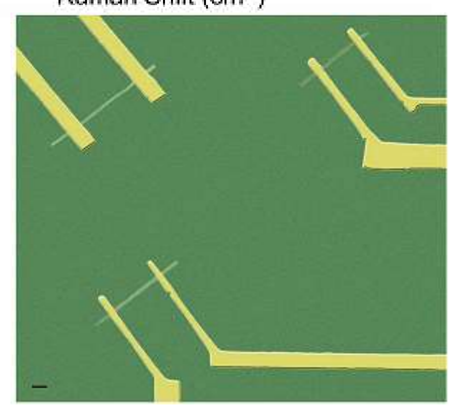

Typical graphene FETs on SiO_2/Si reveal J_{BR} on the order of 10^8 A/cm^2, which is ~100× larger than the limit for the metals but still smaller than the maximum achieved in CNTs

Graphene Interconnects with Increased Breakdown Current Density

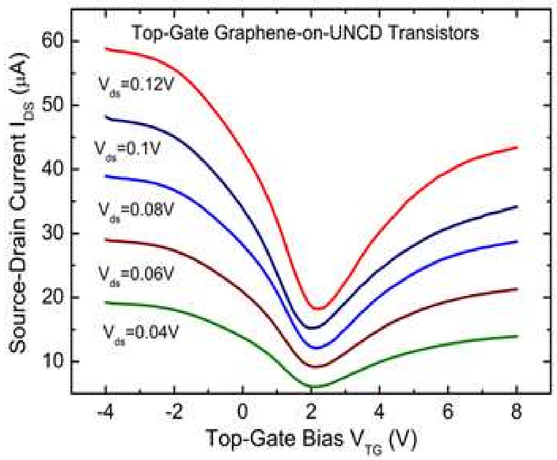

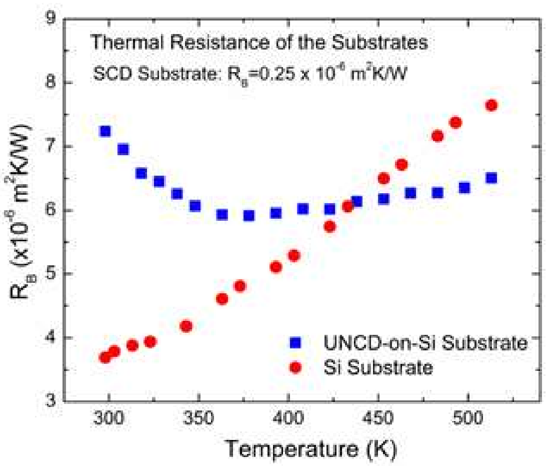

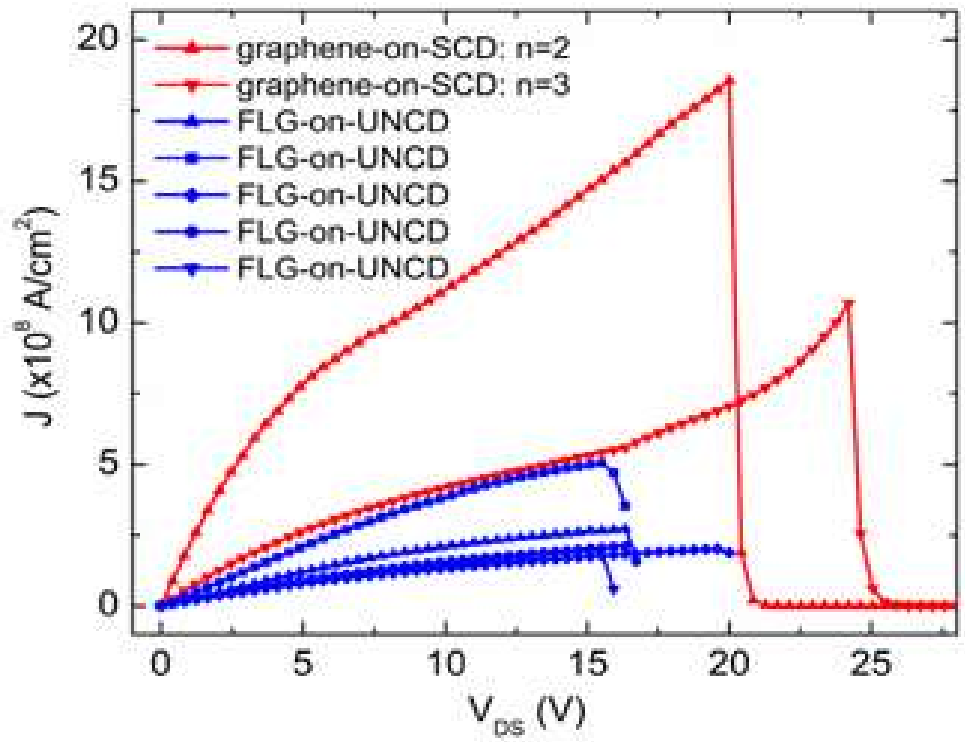

J. Yu, G. Liu, A. Sumant and A.A. Balandin, Graphene-on-diamond devices with increased current-carrying capacity: Carbon sp^2-on-sp^3 technology, *Nano Letters,* 12, 1603 (2012).

Van der Waals Materials: Two-Dimensional Materials Beyond Graphene

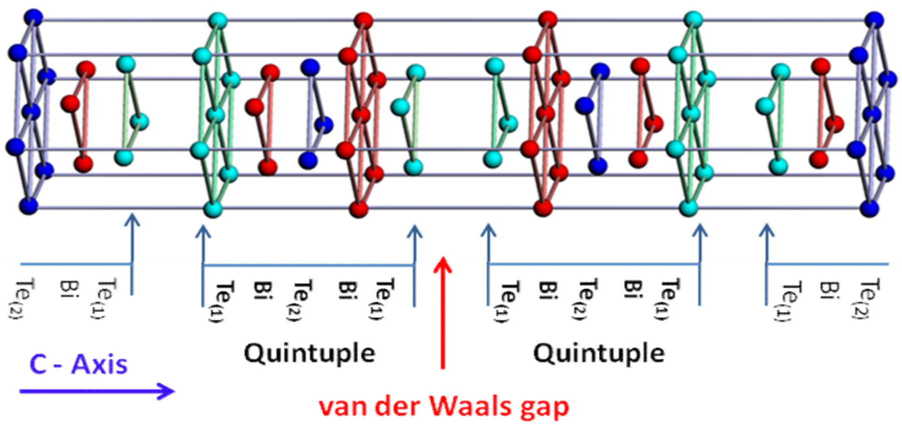

Topological Insulators
→ Benefits of Few-Quintuple Films
→ Predicted High Thermoelectric Figure of Merit

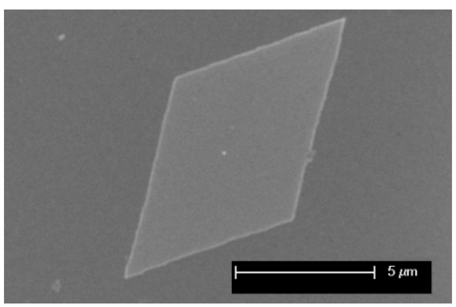

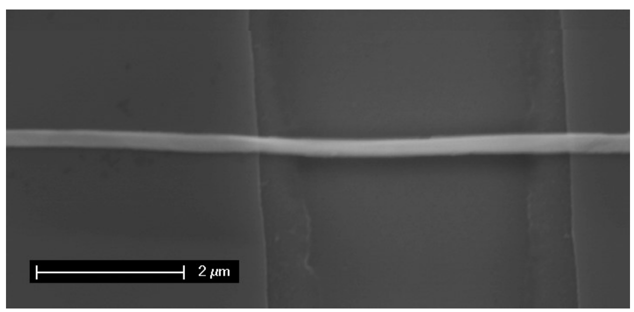

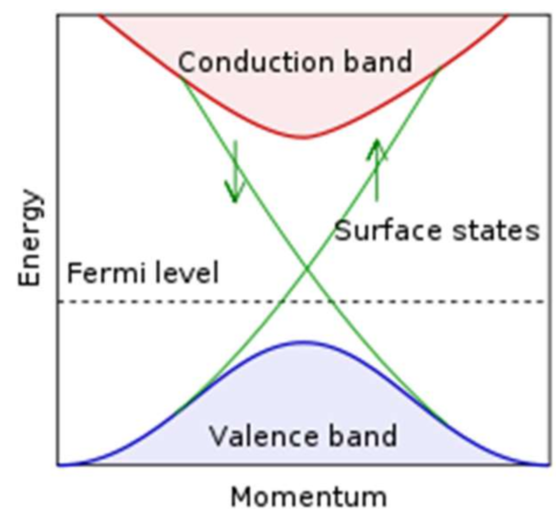

D. Teweldebrhan, V. Goyal and A.A. Balandin, "Exfoliation and characterization of bismuth telluride atomic *quintuples* and quasi-2D crystals," *Nano Letters*, 10, 1209 (2010).

Thermoelectric Motivation for Atomically Thin Films of Bi_2Te_3

The thermoelectric figure of merit: $ZT=S^2\sigma T/(K_e+K_p)$

S is the Seebeck coefficient, σ is the electrical conductivity and *K* is the thermal conductivity.

Electron Quantum Confinement

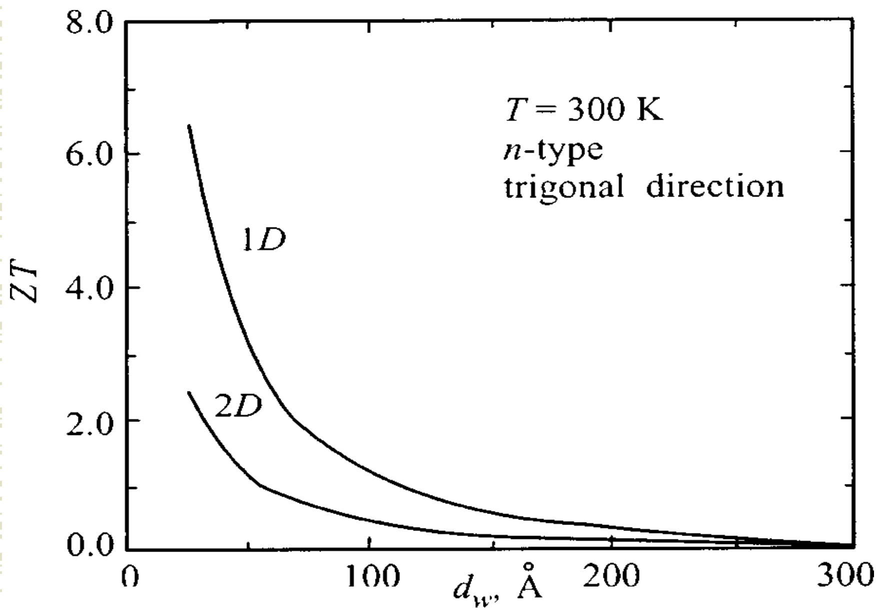

M.S. Dresselhaus, et al. *Phys. Solid State* (1999).
L.D. Hicks and M.S. Dresselhaus, *Phys. Rev. B* (1993).

Acoustic Phonon Confinement

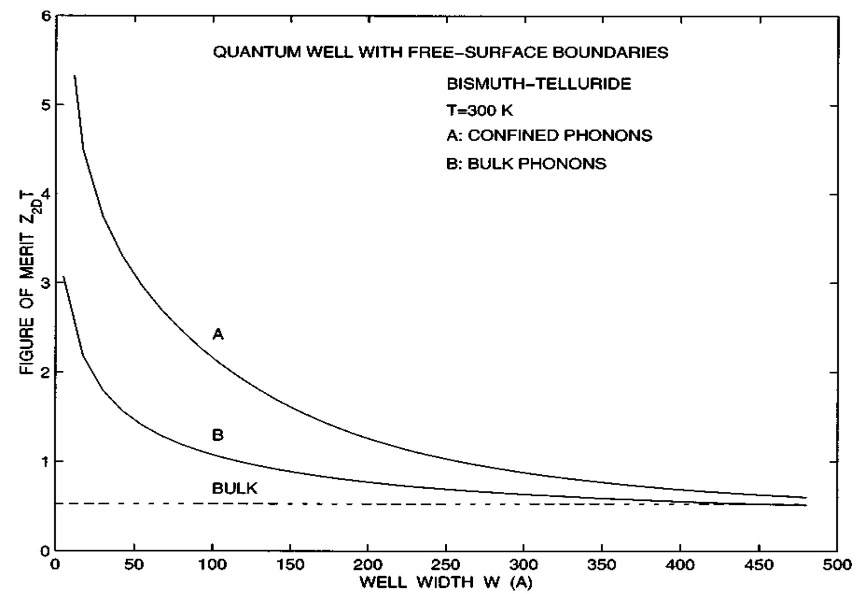

A.A. Balandin and K.L. Wang, *Phys. Rev. B* (1998).
A.A. Balandin and K.L. Wang, *J. Appl. Phys.* (1998).

Low potential barrier in Bi_2Te_3/Bi_2Se_3; Bi_2Te_3/Sb_2Te_3

Raman Spectroscopy of the Atomically Thin Films of Bismuth Telluride

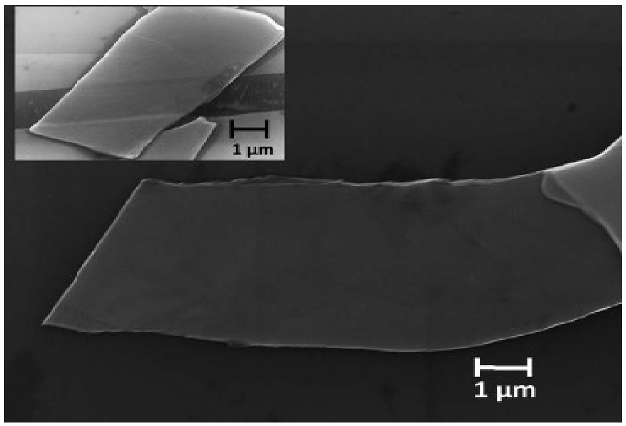

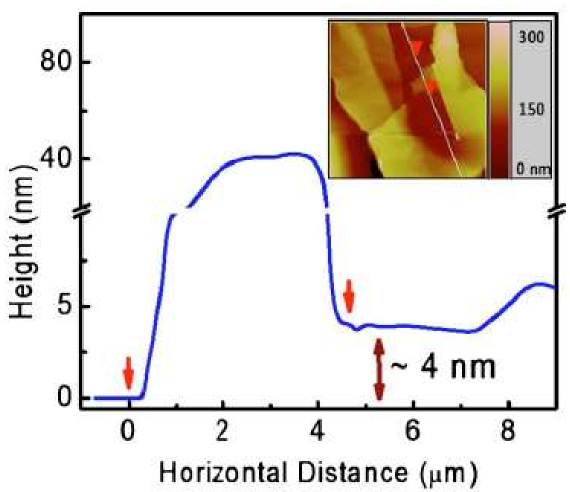

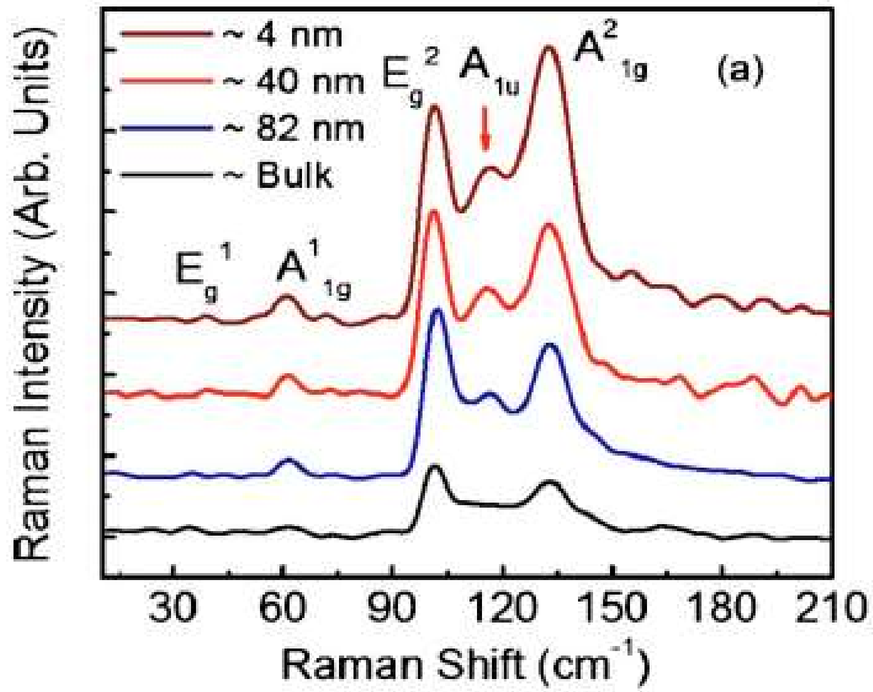

K.M.F. Shahil, M.Z. Hossain, D. Teweldebrhan and A.A. Balandin, "Crystal symmetry breaking in few-quintuple Bi_2Te_3 films: Applications in nanometrology of topological insulators," *Appl. Phys. Lett.*, **96**, 153103 (2010).

Room-Temperature Electrical Characterization Bi-Te Atomic Films

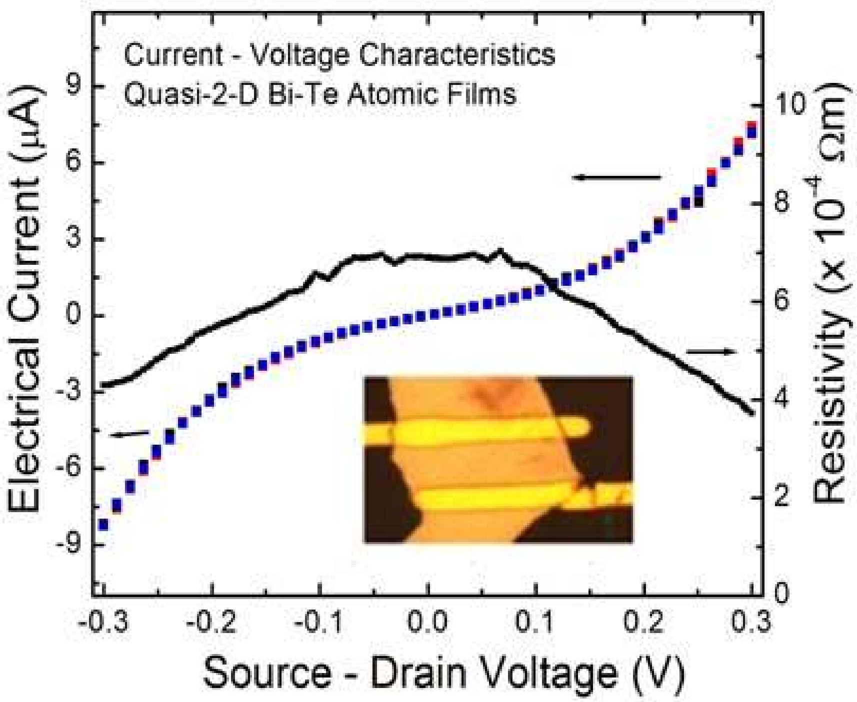

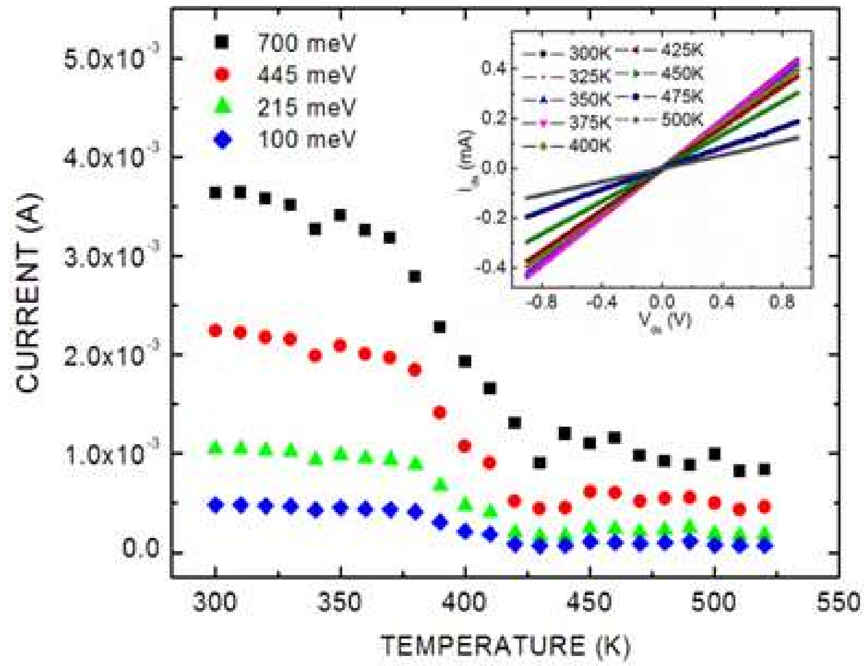

→Weak gating at RT

→ Resistivity is ~10^{-4} Ωm

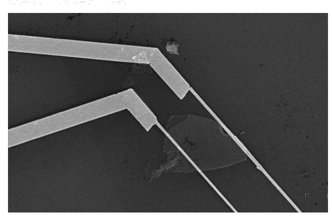

D. Teweldebrhan, V. Goyal, M. Rahman and A.A. Balandin, "Atomically-thin crystalline films and ribbons of bismuth telluride," *Appl. Phys. Lett.*, **96**, 053107 (2010).

Thermoelectric Energy Conversion with Stacks of Bi_2Te_3 Exfoliated Films

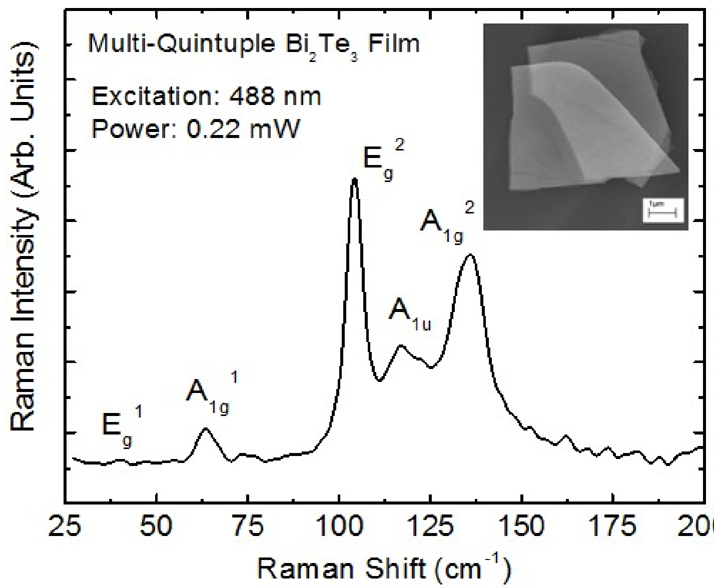

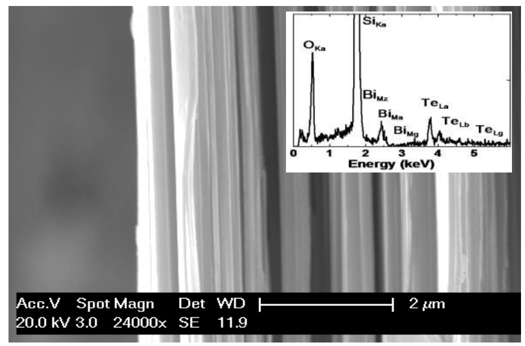

V. Goyal, D. Teweldebrhan and A.A. Balandin, "Mechanically exfoliated stacks of thin films of Bi_2Te_3 topological insulator films", Appl. Phys. Lett. (2010).

ZT increase by ~140 – 250% at room temperature

The enhancement is expected to be larger at low T

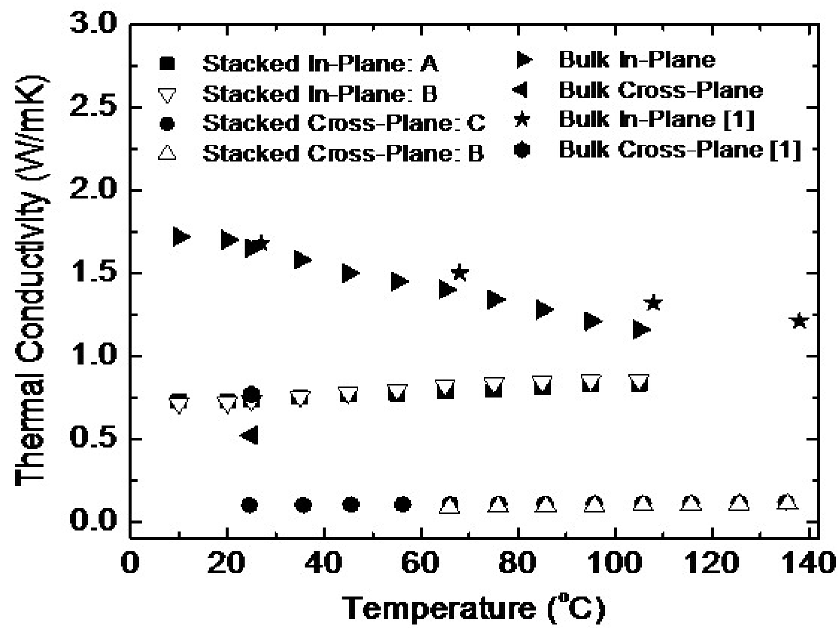

Raman Metrology of Thin Films of Transition Metal Dichalcogenides

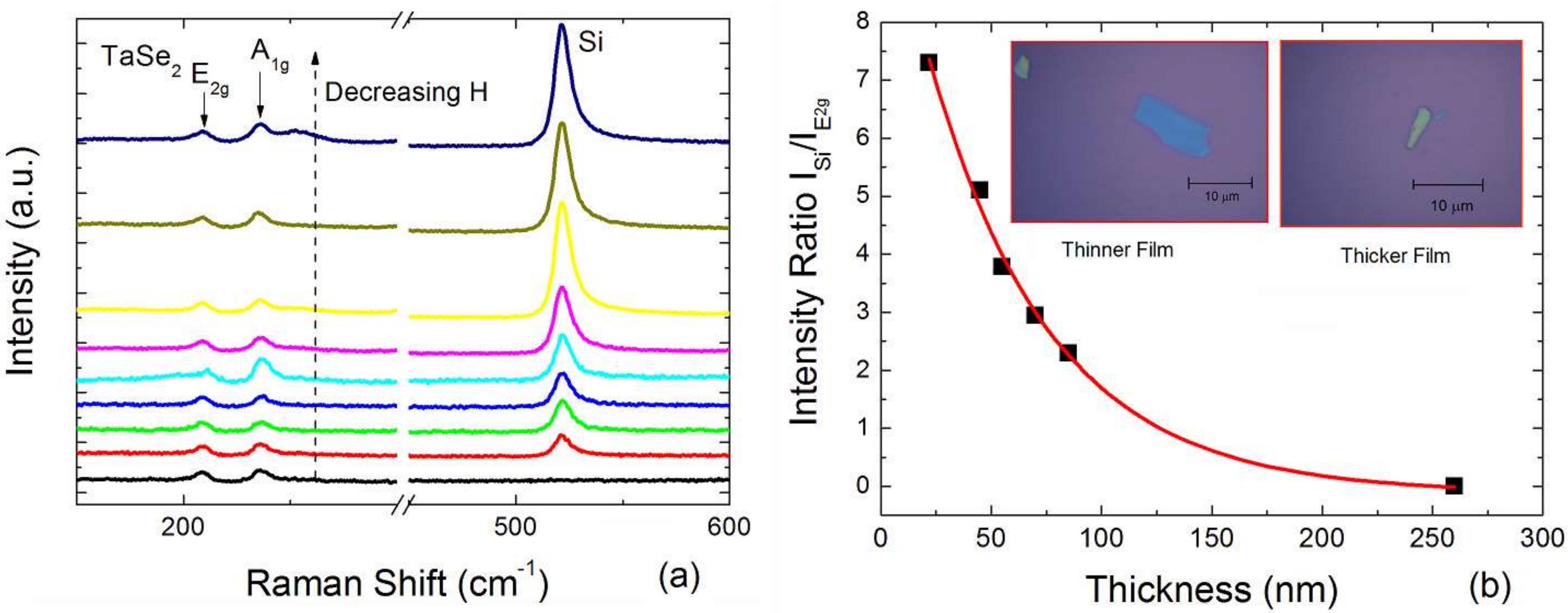

Z. Yan, C. Jiang, T.R. Pope, C.F. Tsang, J.L. Stickney, P. Goli, J. Renteria, T.T. Salguero and A.A. Balandin, “Phonon and thermal properties of exfoliated $TaSe_2$ thin films,” J. Applied Physics, 114, 204301 (2013)

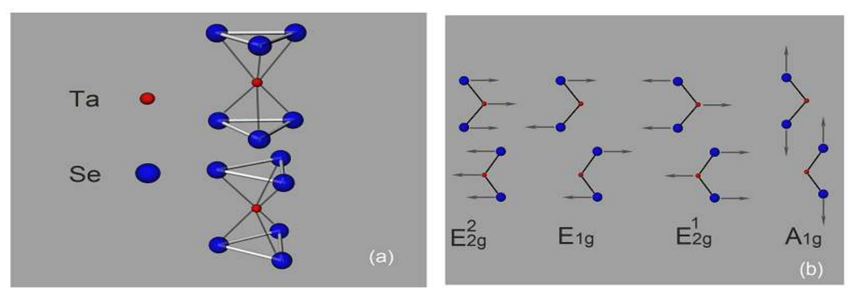

Temperature Dependent Raman Characterization of $TaSe_2$ Thin Films

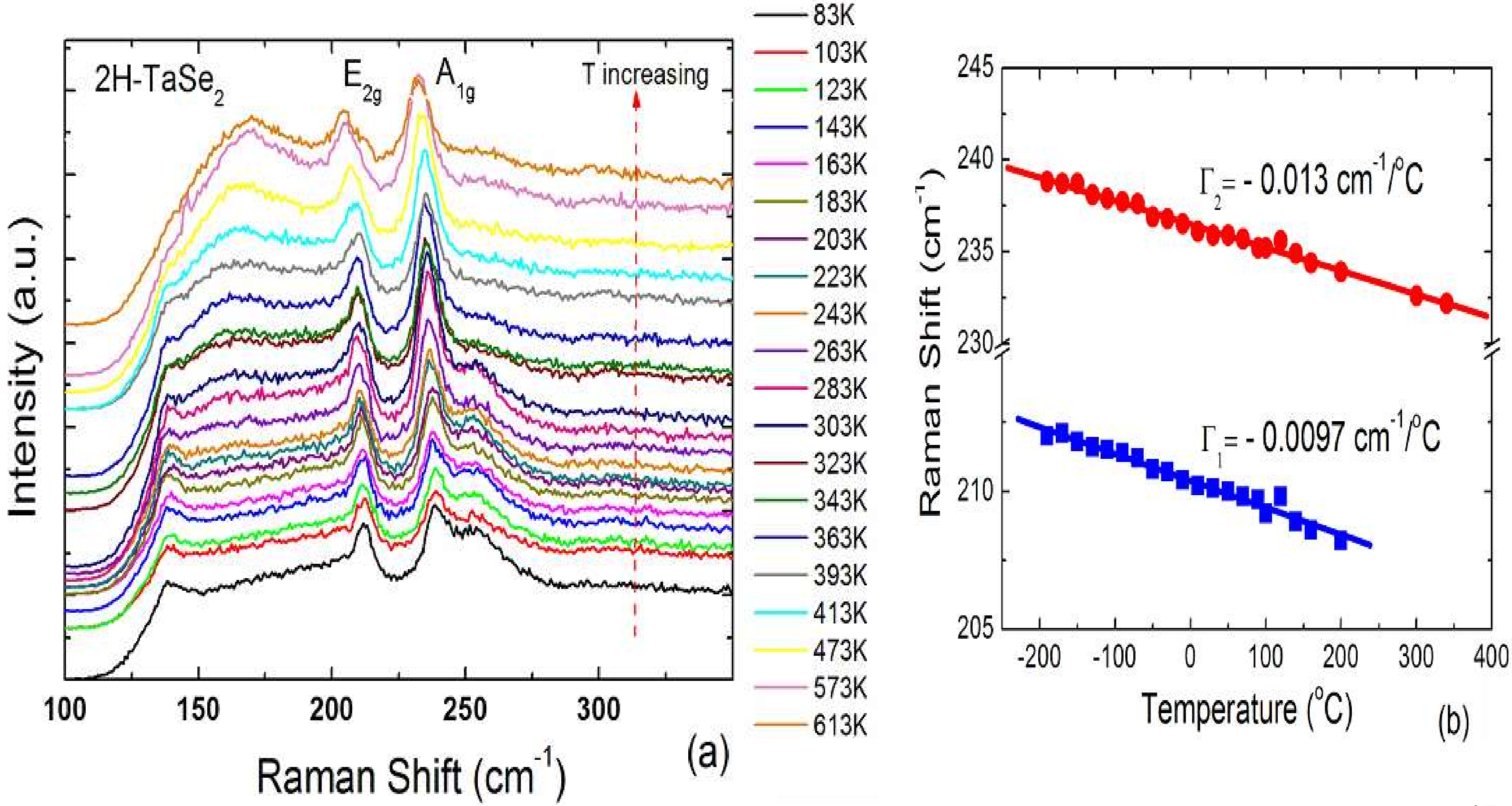

λ=633 nm 2H-$TaSe_2$ T_P=122 K (90 K)

Thermal Properties of Layered Transition Metal Dichalcogenides

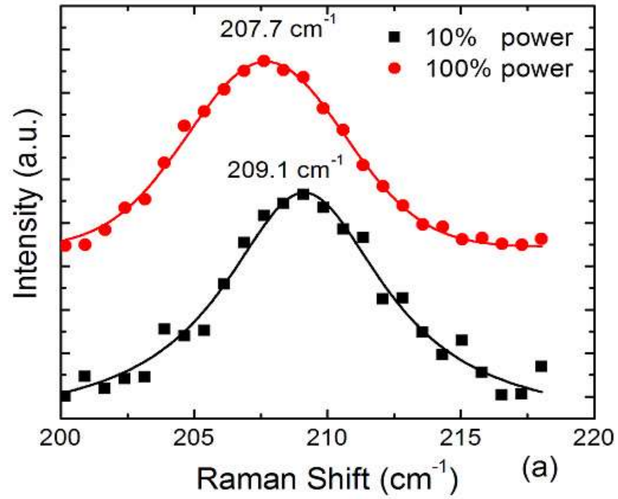

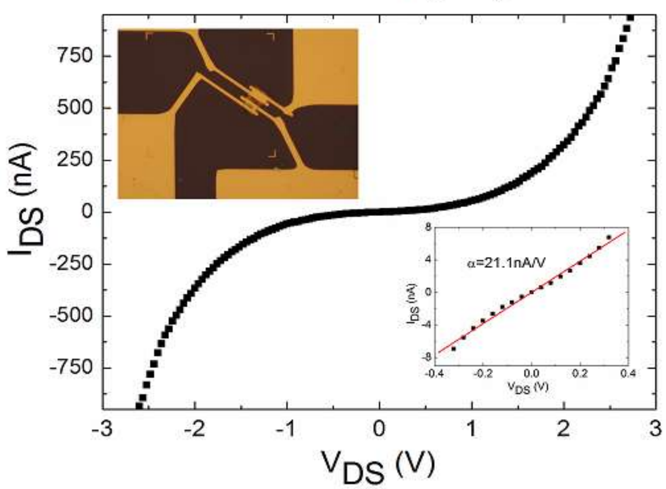

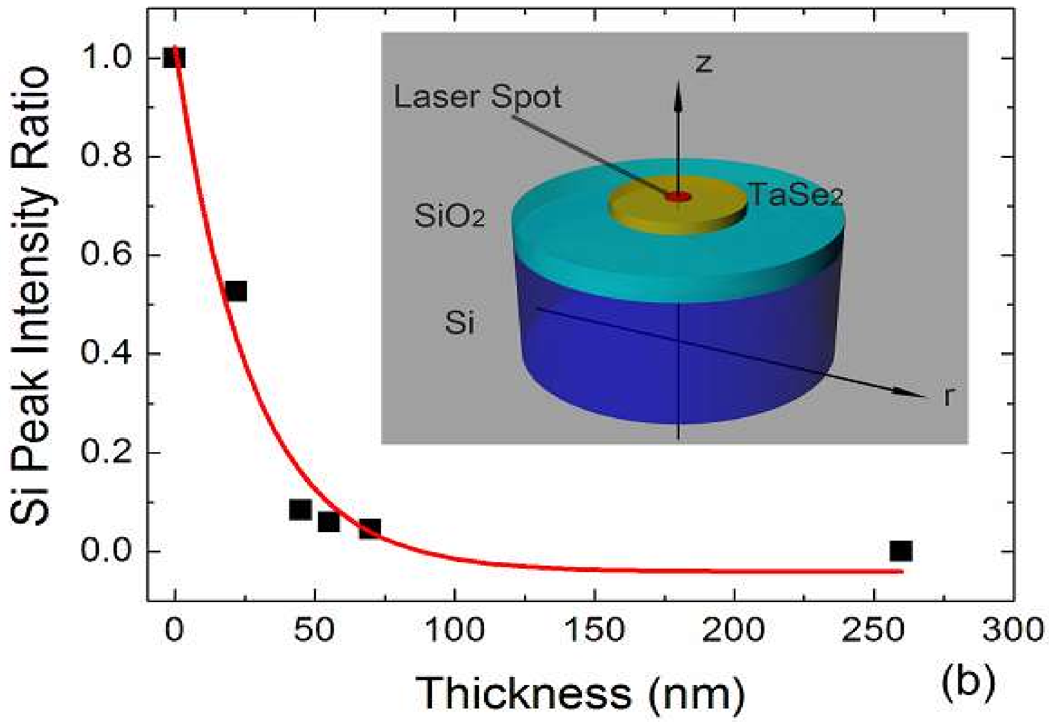

Thickness H (nm)	45	55	85	Bulk
K (W/mK)	9	11	16	16

Phonon Spectrum Evolution with the $TiSe_2$ Film Thickness

| Nano-Device Laboratory >

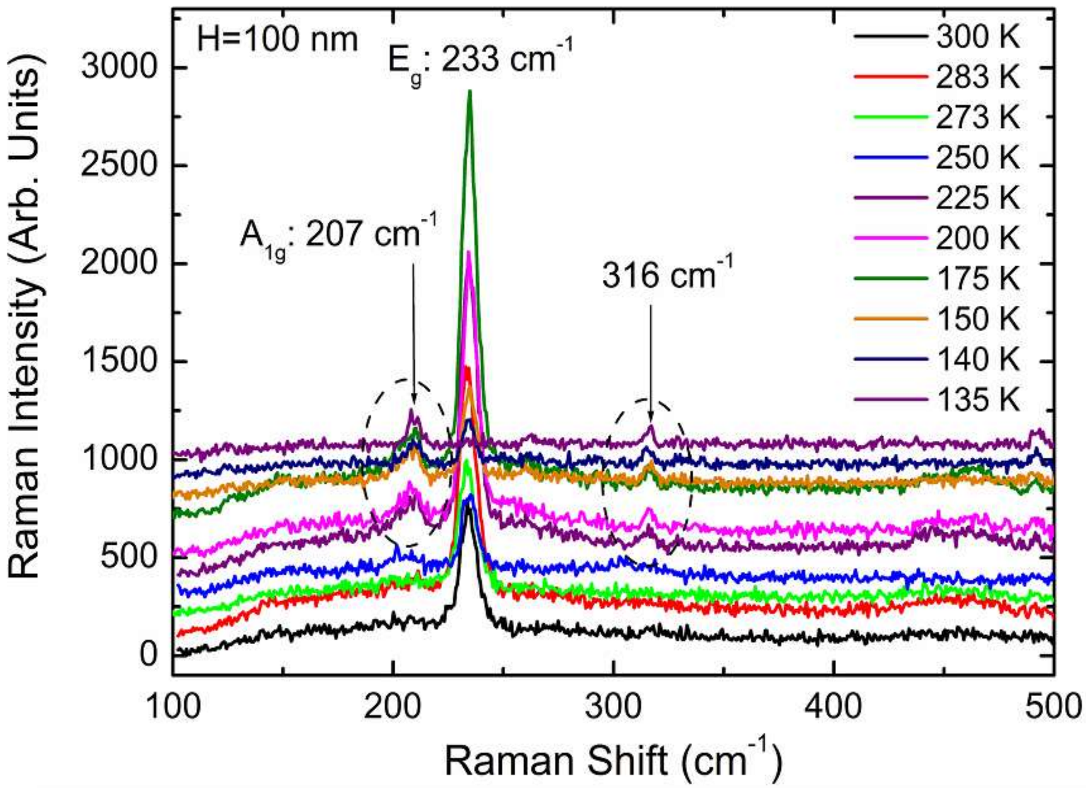

- → Main features are A_{1g} peak at ~207 cm^{-1} and E_g peak at 233 cm^{-1}
- → Peak at 316 cm^{-1} is more pronounced and appears near T_C
- → Temperature at which the spectrum modification is observed is shifter to about ~225 K.
- → Intensity of the low-T Raman peaks varies from sample to sample
- → Emergence of the new Raman lines in $TiSe_2$ is explained by formation of the CDW superlattice below the phase transition temperature

P. Goli, J. Khan, D. Wickramaratne, R.K. Lake and A.A. Balandin, Charge density waves in exfoliated films of van der Waals materials: Evolution of Raman spectrum in $TiSe_2$, Nano Letters, 12, 5941 (2012).

CDW Transition Temperature Scaling with Decreasing Thickness

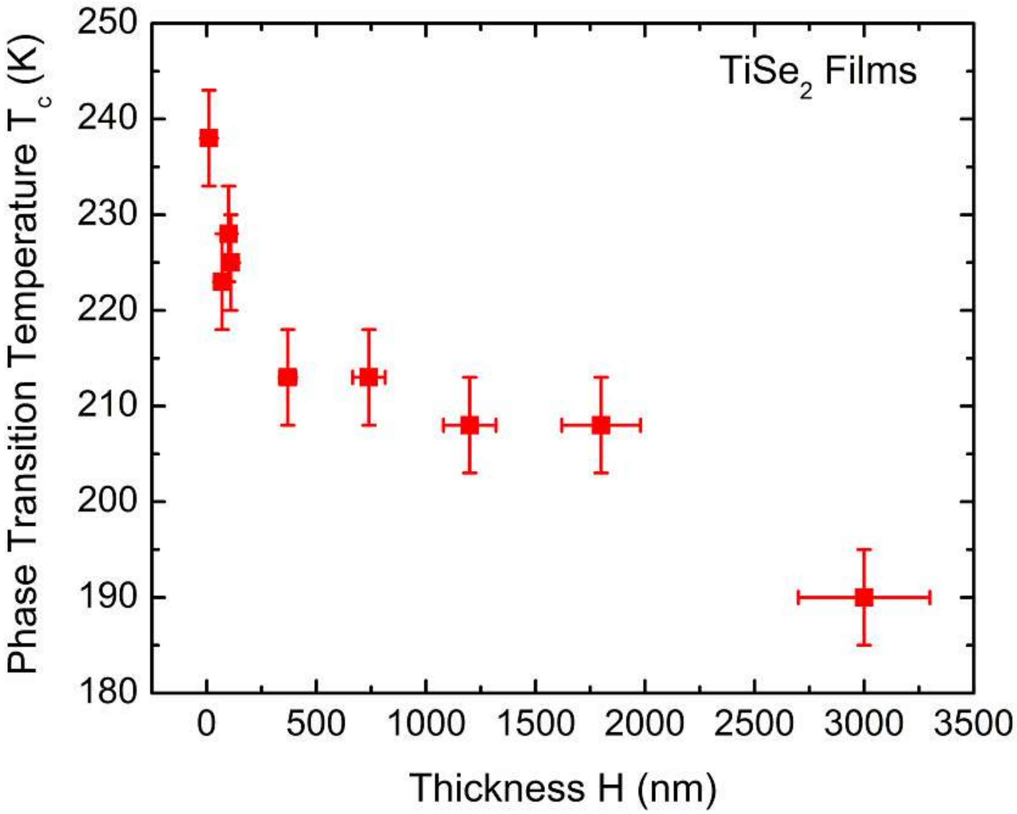

→ CDW transition temperature vs. thickness of the exfoliated $TiSe_2$ thin films.

→ temperature increases from ~200 K in the thick films (H~2 μm) to ~240 K in the thin films (H~100 nm).

→ Major benefit for the proposed electronic applications

Recent theoretical work: M. Calandra, et al., PRB, 80, 241108 (2009)

P. Goli, J. Khan, D. Wickramaratne, R.K. Lake and A.A. Balandin, Charge density waves in exfoliated films of van der Waals materials: Evolution of Raman spectrum in $TiSe_2$, Nano Letters, 12, 5941 (2012).

nature materials

REVIEW ARTICLE

PUBLISHED ONLINE: 22 JULY 2011 | DOI: 10.1038/NMAT3064

Thermal properties of graphene and nanostructured carbon materials

Alexander A. Balandin

RT Thermal Conductivity of Carbon Materials:

Diamond: 1000 – 2200 W/mK

Graphite: 20 – 2000 W/mK

DLC: 0.1 – 10 W/mK

***a*-C: 0.01 – 1 W/mK**

NCD-MCD: 1 – 1000 W/mK

CNTs: 1000 – 3500 W/mK

Graphene: 2000 – 5000 W/mK

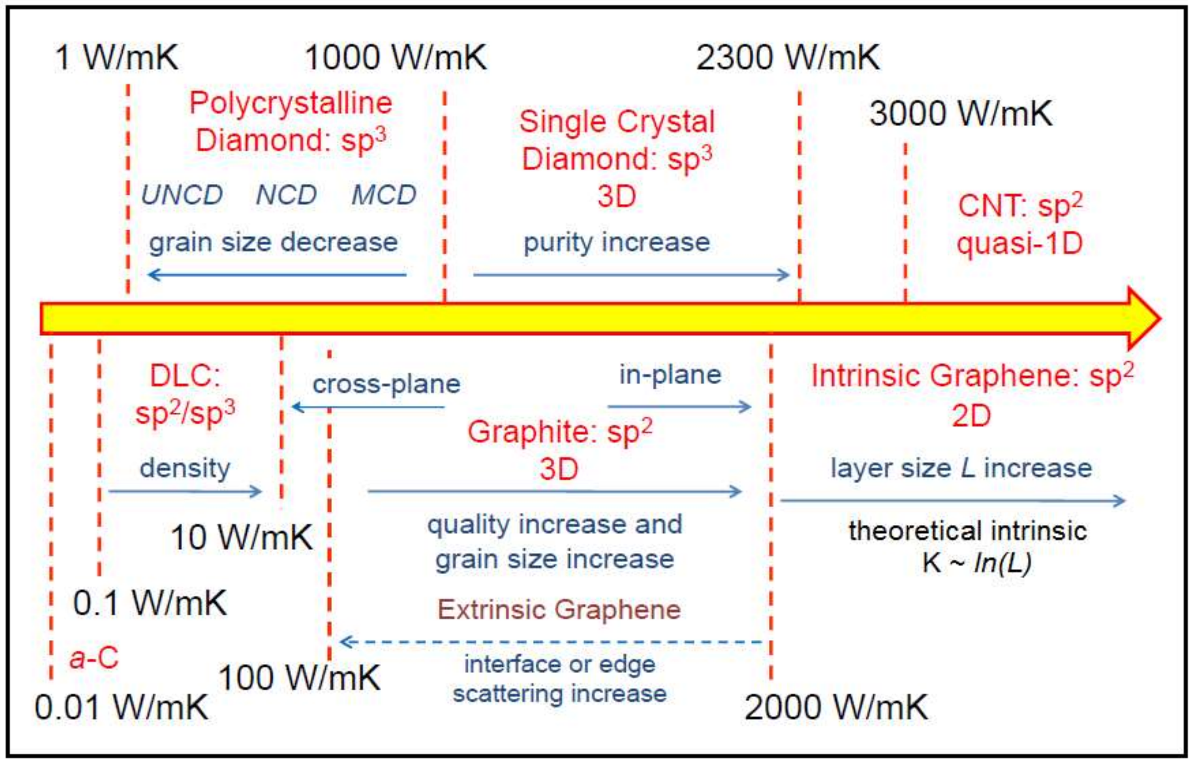

| Nano-Device Laboratory >

Phononics: Beyond "Classical" Size Effects

From Phonon –Boundary Scattering to Phonon Spectrum Engineering

"Classical" size effects on heat conduction: phonon – boundary scattering

Casimir (1938), Berman (1955), Ziman (1960)

Phonon – boundary scattering rate:

$$\frac{1}{\tau_B} = \zeta \frac{1-p}{1+p} \frac{<\upsilon>}{L}$$

PHYSICAL REVIEW B VOLUME 58, NUMBER 3 15 JULY 1998-I

Significant decrease of the lattice thermal conductivity due to phonon confinement in a free-standing semiconductor quantum well

Alexander Balandin and Kang L. Wang
Device Research Laboratory, Electrical Engineering Department, University of California–Los Angeles, Los Angeles, California 90095-1594

(Received 17 February 1998; revised manuscript received 20 April 1998)

Tuning thermal conductivity can be approached with appropriate modification of phonon modes, e.g., phonon engineering.

Phononics: From Bulk to Nanostructures to 2D Materials

Bulk Semiconductor

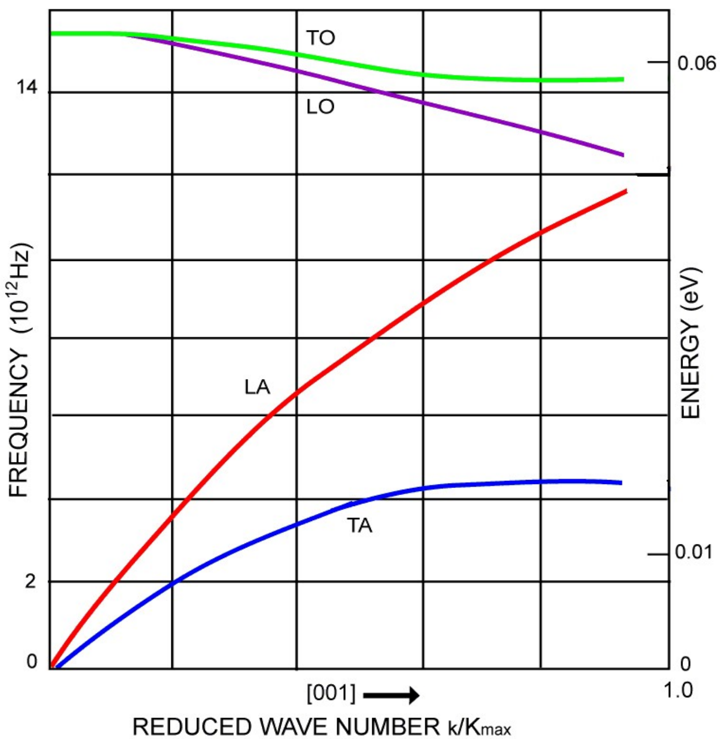

E.P. Pokatilov, D.L. Nika and A.A. Balandin, "Acoustic-phonon propagation in semiconductor nanowires with elastically dissimilar barriers," *Physical Review B*, **72**, 113311 (2005)

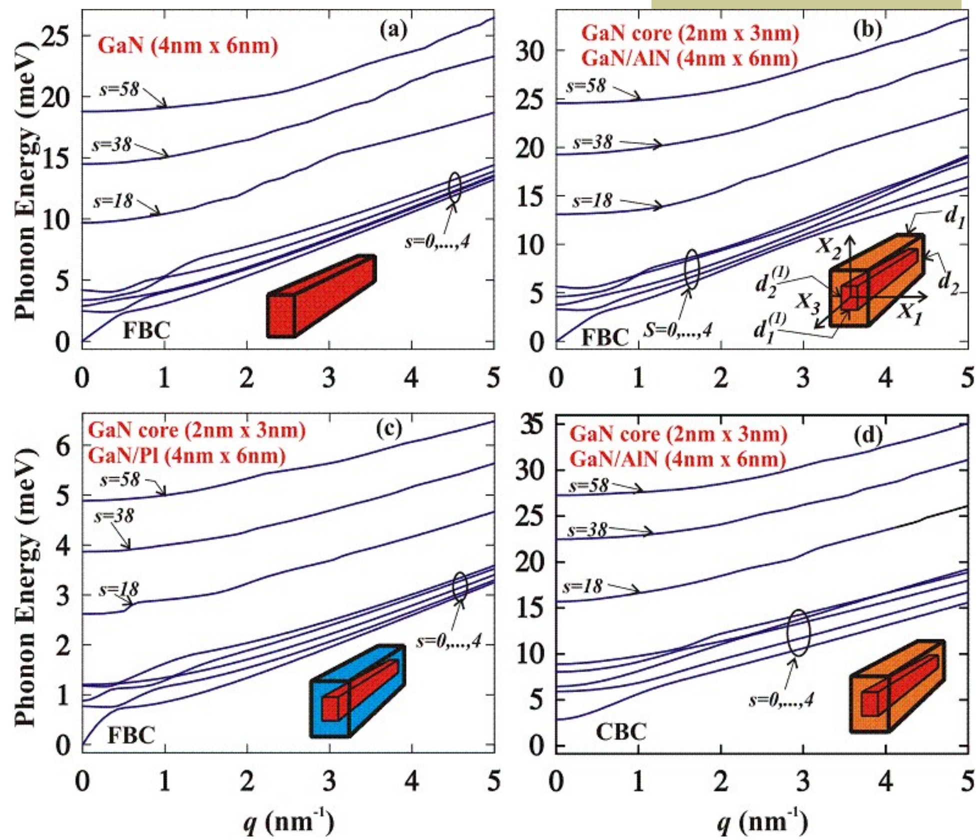

D.L. Nika, E.P. Pokatilov and A.A. Balandin, "Phonon - engineered mobility enhancement in the acoustically mismatched transistor channels," *Appl. Phys. Lett.*, **93**, 173111 (2008).

Engineering Phonons by Twisting Atomic Planes

Phonons in Twisted Bilayer Graphene

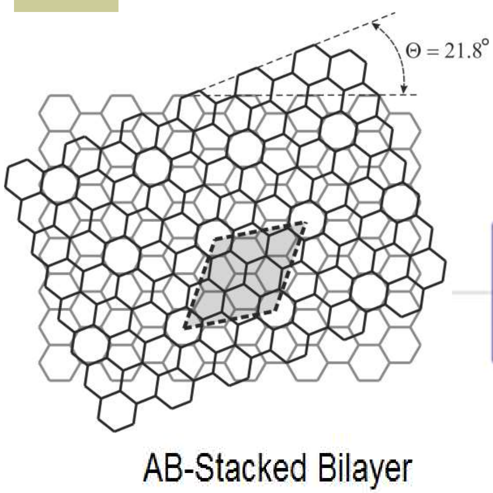

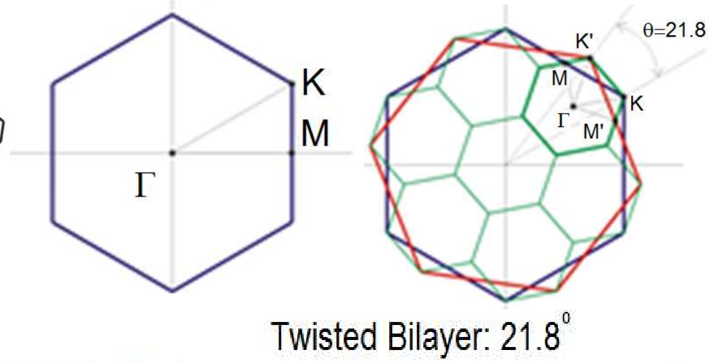

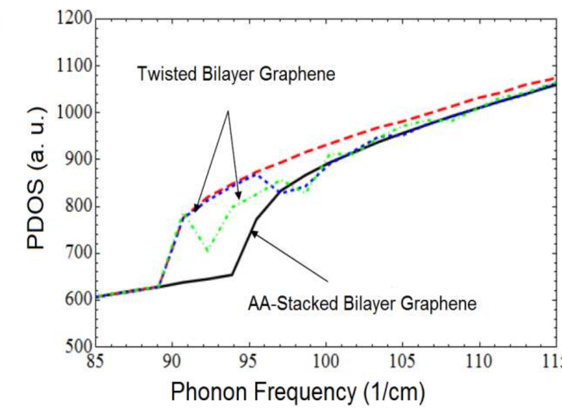

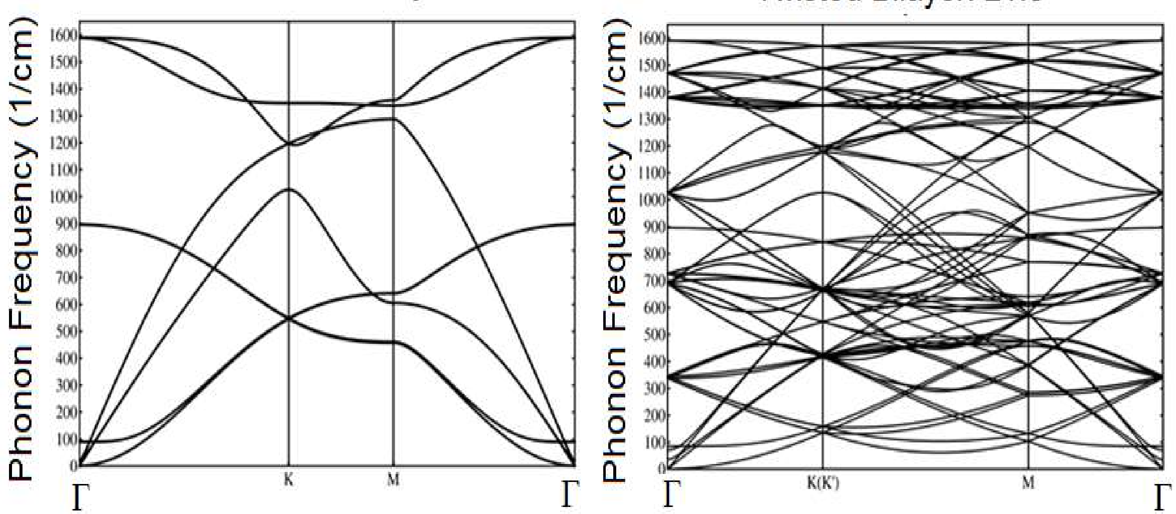

- → Born-von Karman model for description of the carbon-carbon intra-layer interactions
- → Lennard-Jones potential for the inter-layer interactions

A.I. Cocemasov, D.L. Nika and A.A. Balandin, "Phonons in twisted bilayer graphene" Phys. Rev. B, 88, 035428 (2013)],

Saving the Fourier Law

Intrinsic Thermal Conductivity of 2D Crystals

Graphene: 2-D hexagonal honeycomb lattice of sp^2-bound carbon atoms

Intrinsic: no scattering on edges or defects

No boundaries

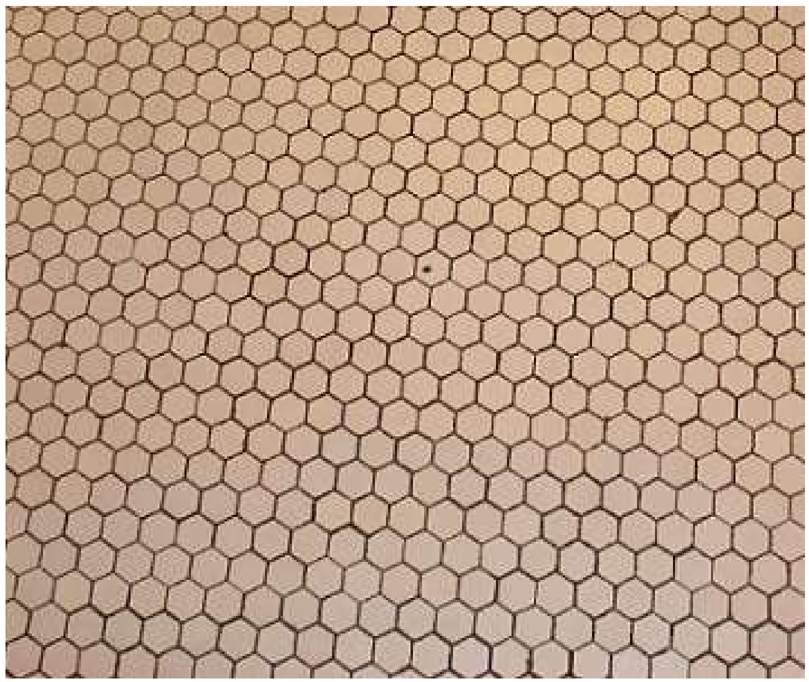

No boundaries

Alexander A. Balandin, University of California – Riverside

Real Systems Have Finite Size and Defects

Graphene: 2-D hexagonal honeycomb lattice of sp^2-bound carbon atoms

"Graphene" tiles "discovered" in the historic *La Fonda Hotel*, Santa Fe, New Mexico

Phononics in Low-Dimensional Materials

- *Thermal conduction in 2D crystals is different from that in 3D bulk owing to specifics of long-wavelength phonon transport*
- *Thermal conductivity of the atomically thin films depends on the interplay of the intrinsic and extrinsic effects*
- *Graphene and van der Waals materials offer new opportunities for phonon engineering*
- *Technology has reached the state required for engineering phonon modes*
- *Strong practical motivation due to the problems of heat removal in a variety of electronic and optoelectronic devices*

A.A. Balandin and D.L. Nika "Phonons in low-dimensions: Engineering phonons in nanostructures and graphene," *Materials Today*, **15** 266 (2012).

A.A. Balandin, "Thermal properties of graphene and nanostructured carbon materials," Nature Materials, 10, 569 - 581 (2011).

Acknowledgements

Nano-Device Laboratory (NDL), UC Riverside, 2010 – 2013

Special thanks to

Prof. E.P. Pokatilov and Prof. D. Nika (Moldova State Univ.)

STARnet

SRC

DARPA

FAME

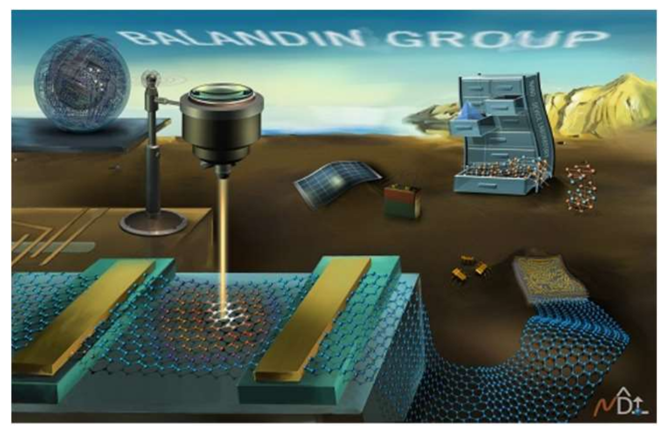

UC RIVERSIDE
UNIVERSITY OF CALIFORNIA


City of Riverside


UCR Bell Tower


UCR Engineering Building


UCR Botanic Gardens


Joshua Tree Park, California